Hypothalamic POMC deficiency increases circulating adiponectin despite obesity

Hui Yu [1,*], Kavaljit H. Chhabra [1,2], Zoe Thompson [1], Graham L. Jones [3], Sylee Kiran [1,4], Gary Shangguan [1], Malcolm J. Low [1,3]

ABSTRACT

Objective: The steep rise in the prevalence of obesity and its related metabolic syndrome have become a major worldwide health concerns. Melanocortin peptides from hypothalamic arcuate nucleus (Arc) POMC neurons induce satiety to limit food intake. Consequently, Arc *Pomc*-deficient mice (Arc*Pomc*$^{-/-}$) exhibit hyperphagia and obesity. Previous studies demonstrated that the circulating levels of adiponectin, a protein abundantly produced and secreted by fat cells, negatively correlate with obesity in both rodents and humans. However, we found that Arc*Pomc*$^{-/-}$ mice have increased circulating adiponectin levels despite obesity. Therefore, we investigated the physiological function and underlying mechanisms of hypothalamic POMC in regulating systemic adiponectin levels.

Methods: Circulating adiponectin was measured in obese Arc*Pomc*$^{-/-}$ mice at ages 4—52 weeks. To determine whether increased adiponectin was a direct result of Arc*Pomc* deficiency or a secondary effect of obesity, we examined plasma adiponectin levels in calorie-restricted mice with or without a history of obesity and in Arc*Pomc*$^{-/-}$ mice before and after genetic restoration of *Pomc* expression in the hypothalamus. To delineate the mechanisms causing increased adiponectin in Arc*Pomc*$^{-/-}$ mice, we determined sympathetic outflow to adipose tissue by assessing epinephrine, norepinephrine, and tyrosine hydroxylase protein levels and measured the circulating adiponectin in the mice after acute norepinephrine or propranolol treatments. In addition, adiponectin mRNA and protein levels were measured in discrete adipose tissue depots to ascertain which fat depots contributed the most to the high level of adiponectin in the Arc*Pomc*$^{-/-}$ mice. Finally, we generated compound *Adiopoq*$^{-/-}$:Arc*Pomc*$^{-/-}$ mice and compared their growth, body composition, and glucose homeostasis to the individual knockout mouse strains and their wild-type controls.

Results: Obese Arc*Pomc*$^{-/-}$ female mice had unexpectedly increased plasma adiponectin compared to wild-type siblings at all ages greater than 8 weeks. Despite chronic calorie restriction to achieve normal body weights, higher adiponectin levels persisted in the Arc*Pomc*$^{-/-}$ female mice. Genetic restoration of *Pomc* expression in the Arc or acute treatment of the Arc*Pomc*$^{-/-}$ female mice with melanotan II reduced adiponectin levels to control littermate values. The Arc*Pomc*$^{-/-}$ mice had defective thermogenesis and decreased epinephrine, norepinephrine, and tyrosine hydroxylase protein levels in their fat pads, indicating reduced sympathetic outflow to adipose tissue. Injections of norepinephrine into the Arc*Pomc*$^{-/-}$ female mice reduced circulating adiponectin levels, whereas injections of propranolol significantly increased adiponectin levels. Despite the beneficial effects of adiponectin on metabolism, the deletion of adiponectin alleles in the Arc*Pomc*$^{-/-}$ mice did not exacerbate their metabolic abnormalities.

Conclusion: In summary, to the best of our knowledge, this study provides the first evidence that despite obesity, the Arc*Pomc*$^{-/-}$ mouse model has high circulating adiponectin levels, which demonstrated that increased fat mass is not necessarily correlated with hypoadiponectinemia. Our investigation also found a previously unknown physiological pathway connecting POMC neurons via the sympathetic nervous system to circulating adiponectin, thereby shedding light on the biological regulation of adiponectin.

1. INTRODUCTION

The central melanocortin system is composed of neurons in the hypothalamic arcuate nucleus (Arc) that express *proopiomelanocortin* (*Pomc*) and release melanocortin and β-endorphin neuropeptides from their axonal projections, and neurons that produce agouti-related peptide (AgRP), an endogenous antagonist of melanocortins [1,2]. This system plays an essential role in the regulation of satiety, glucose homeostasis, and energy expenditure [3—5]. Deficiencies in central *Pomc* gene expression and the production of melanocortin peptides or dysfunction of melanocortin 4 receptor induce severe hyperphagia and decreased energy expenditure leading to obesity [6—10]. In addition to

[1]Department of Molecular and Integrative Physiology, University of Michigan Medical School, Ann Arbor, MI, 48105, USA [2]Department of Medicine, Division of Endocrinology, Diabetes and Metabolism, University of Rochester School of Medicine and Dentistry, Rochester, NY, USA [3]Neuroscience Graduate Program, University of Michigan, Ann Arbor, MI, USA [4]School of Literature, Science, and Arts, University of Michigan, Ann Arbor, MI, USA

*Corresponding author. Department of Molecular and Integrative Physiology, University of Michigan, Brehm Tower, Room 6430, 1000 Wall St., Ann Arbor, MI, 48105. E-mail: huiyuz@umich.edu (H. Yu).

List of abbreviations

Pomc	Proopiomelanocortin gene
Arc	arcuate nucleus
Arc*Pomc*$^{-/-}$/*Pomc* null	*Pomc* inactivation specifically in arcuate nucleus
SNS	sympathetic nervous system
ANOVA	analysis of variance
MTII	melanotan II
MC3R/MC4R	melanocortin 3/melanocortin 4 receptor
MSH	melanocyte-stimulating hormone
ACTH	adrenocorticotropic hormone
TH	tyrosine hydroxylase
Arc*Pomc*$^{-/-}$:*Adipoq*$^{-/-}$	deletion of adiponectin in Arc*Pomc*$^{-/-}$ mice

the regulation of appetite, POMC neurons also have indirect effects on adipose tissue function. For example, mice with POMC neuron specific deficiency of *Ire1α* (*inositol-requiring enzyme 1*) exhibited impaired thermogenic responses in both brown fat and inguinal fat in response to cold exposure [11]. Deletion of *Atg7* (*autophagy related 7*) in POMC neurons resulted in a failure of lipid utilization in brown fat during fasting and cold exposure [12]. Furthermore, POMC neuron specific deletion of the tyrosine phosphatase proteins TCPTP and PTP1B resulted in decreased fat mass in epididymal and subcutaneous fat pads and enhanced thermogenesis in both brown and subcutaneous fat depots with no changes in food intake and overall body weight [13]. A unifying mechanism of these phenotypes is the modulation of sympathetic outflow from the CNS to peripheral tissues by POMC neuron activity. Many studies have shown that brown adipose tissue is densely innervated with sympathetic nerves that regulate thermogenesis [14]. In addition, a recent study using volume fluorescence imaging revealed that more than 90% of inguinal adipocytes also exhibited innervation by sympathetic nerve fibers [15]. Using retrograde tracing and *in situ* hybridization, MC4R was found to be extensively expressed in the pre-sympathetic motor neurons of the spinal cord intermediolateral column that project via sympathetic post-ganglionic neurons to both brown and inguinal white adipose tissues [16–18]. Similarly, POMC neurons in the Arc have been shown to project transynaptically to brown fat [19]. The major function of the sympathetic nervous system (SNS) in adipose tissue is to govern energy homeostasis through its control of thermogenesis, lipolysis, lipid mobilization, and regulation of leptin production and secretion [20,21]. However, the role of the SNS in regulating other circulating adipokines, such as adiponectin, is less well defined.

Adiponectin is a 244-amino acid protein produced and secreted almost exclusively by adipocytes [22]. The concentration of adiponectin in the circulation is high both in humans and mice and is sexually dimorphic. Generally, females have higher levels than males, probably due to the effects of the sex steroids, testosterone, and estrogen [23,24]. Adiponectin is synthesized as a monomer of 28–30 kDa and is later assembled into homo-oligomers with various molecular weights: the trimeric form with a low molecular weight (LMW), the hexameric form with a medium molecular weight (MMW), and the multimeric form (12–18 mer) with a high molecular weight (HMW) [25,26]. Among them, the HMW form has been implicated as the most biologically active form for insulin sensitivity and a reduction in HMW oligomers is associated with diabetes in humans [27–30] and mice [31]. Since adiponectin was first identified in the 1990s, it has attracted attention because of its positive action on metabolic homeostasis. Adiponectin

targets key organs, including muscle, pancreas, liver, adipose tissue, and brain, to regulate glucose metabolism and insulin action. Adiponectin has been shown to reduce the risks of metabolic syndrome [32], chronic kidney diseases [33–35], atherosclerosis [36,37], diabetic retinopathy [35], and certain cancers [38]. Moreover, the gene encoding human adiponectin (*Adipoq*) is located on chromosome 3 in the 3q27 region, a loci that has been reported in GWAS analyses as highly associated with metabolic syndrome and type 2 diabetes [39,40]. Mutations in human *Adipoq* increase the risk of pathogenesis of type 2 diabetes [41–43]. In addition, increasing circulating adiponectin either by genetic modification or vector administration significantly improved glucose tolerance, insulin sensitivity, and other metabolic measures in mice [44–46], although mouse models with *Adipoq null* alleles were viable [47–49] and shared similar body weights, fat mass, glucose tolerance, and insulin sensitivity as wild-type control mice on a normal chow diet.

Unlike leptin, whose circulating levels positively correlate with fat mass, circulating adiponectin is greatly reduced in both diet-induced and genetic animal models of obesity [45,50–52] and in obese and insulin-resistant humans [51,53]. Therefore, pharmacological elevation of circulating adiponectin may offer a promising avenue to ameliorate obesity and its related diseases. Studies have shown that the insulin-sensitizing effects of the PPARγ agonists thiazolidinediones, such as rosiglitazone and pioglitazone, are partially mediated by elevated circulating levels of adiponectin in humans [54]. In our previous studies, we developed a mouse model with disruption of the two distal neuronal *Pomc* enhancers nPE1 and nPE2 [6]. *Pomc* expression in the hypothalamus was reduced by ∼99%, whereas its expression in the pituitary remained intact. These Arc*Pomc*$^{-/-}$ mice were hyperphagic and severely obese with hyperleptinemia. However, our initial attempt to phenotype this mouse model revealed a surprisingly increased level of circulating adiponectin despite morbid obesity and insulin resistance. Caron et al. reported that a subset of POMC neurons that express leptin receptors are necessary to regulate leptin synthesis independent of changes in fat mass [20]. Because leptin and adiponectin are both adipokines produced and secreted from adipose tissue and their circulating levels are associated with fat mass, we speculate that reduced *Pomc* expression would have an effect on adiponectin levels. Based on our initial discoveries, the current study further investigated the potential role of POMC neurons in regulating circulating adiponectin. We found that elevated circulating adiponectin in Arc*Pomc*$^{-/-}$ mice exhibited a sex- and *Pomc*-expression-dependent profile. Reduced sympathetic outflow to subcutaneous fat depots at least partially contributes to this alteration in adiponectin homeostasis.

2. MATERIALS AND METHODS

2.1. Animal care

All of the procedures were conducted in accordance with the Institutional Animal Care and Use Committee (IACUC) at the University of Michigan and followed the Public Health Service guidelines for the humane care and use of experimental animals. Mice were housed in ventilated cages under controlled temperatures and photoperiods (12-hour light/12-hour dark cycle, lights on from 6:00 am to 6:00 pm) with free access to tap water and laboratory chow (5L0D, LabDiet) containing 28.67% protein, 13.38% fat, and 57.94% carbohydrate by weight available *ad libitum*. Breeding mice were fed a breeder chow diet (5008, LabDiet) containing 26.53% protein, 16.97% fat, and 56.50% carbohydrates. Arc*Pomc*$^{-/-}$ and *Pomc*-CreERT:Arc*Pomc*$^{-/-}$ mice were generated and bred as previously described [6,55,56].

$Adipoq^{-/-}$ mice were obtained from the Jackson Laboratory (Stock #: 008195) and cross-bred with Arc$Pomc^{+/-}$ females to generate animals with mutations in both alleles.

2.2. General procedures for animal experiments

Weight-matched experiments were conducted by individually housing and feeding the Arc$Pomc^{-/-}$ mice 70%—75% of the daily food intake of their wild-type littermates. Animal health was checked every day and their body weights were measured twice a week. Their food intake was adjusted accordingly to ensure all the obese animals had a steadily gradual weight loss. To reactivate $Pomc$ expression in the $Pomc$-CreERT:Arc$Pomc^{-/-}$ mice, tamoxifen (50 mg/kg) was injected intraperitoneally for each of five consecutive days as previously described [57]. The same treatment was also performed on their littermate control mice ($Pomc$-CreERT:Arc$Pomc^{+/+}$). For all of the pharmacological treatment experiments, the mice were handled and injected with saline every day for a week before any drug administration to acclimate them to handling. The vehicle and drug treatments were conducted on the same animals separated by one week. Tail blood samples were acquired at indicated time points. All of the drugs were administrated intraperitoneally at the following doses: melanotan II (MTII, Sigma—Aldrich, M8693); 100 μg/animal; norepinephrine: 2.5 mg/kg body weight; and propranolol: 3.5 mg/kg body weight. Norepinephrine was dissolved in 100 μM ascorbic acid to avoid fast oxidation, and both MTII and propranolol were dissolved in 0.9% saline solution. Animal body composition was assessed by nuclear magnetic resonance using the Bruker Minispec LF 90II at the University of Michigan Metabolism, Bariatric Surgery, and Behavior Core.

2.3. Cell culture

Ear mesenchymal stem cells (EMSC) were isolated and differentiated in culture as previously described [58,59]. Fully differentiated EMSCs were treated with vehicle (PBS) or MTII at varying concentrations. 3T3-L1 adipogenesis was conducted as previously described [60]. Approximately 70% confluent cells were induced to differentiation with 10% FBS with 0.5 mM methylisobutylxanthine, 1 μM dexamethasone, and 1 μg/mL insulin. On day 2, the cells were fed 1 μg/mL insulin in 10% FBS, and on day 4 and every 2 days thereafter, the cells were fed with 10% FBS. Fully differentiated cells were treated with adrenocorticotropic hormone (ACTH, Phoenix Pharmaceuticals, 001—21) dissolved in 5% acetic acid solution at different doses. An aliquot of 50 μl of medium was collected at indicated time points for adiponectin measurement.

2.4. Gene expression and immunoblotting analysis

Total adipose tissue RNA was extracted using TRIzol (Thermo Fisher Scientific, 15596026) as described by the manufacturer. cDNA was obtained by reverse transcription of 2 μg RNA with random primers using M-MLV Reverse Transcriptase (Thermo Fisher Scientific, 28025013). qRT-PCR was performed on all the samples using a StepOne Real-Time PCR System (Applied Biosystems) and SYBR Green Master Mix (Life Technologies). The following primers were used to detect adiponectin: (forward: 5′-TGTTCCTCTTAATCCTGCCCA-3′; reverse: 5′-CCAACCTGCACAAGTTCCCTT-3′), reference gene *TATA binding protein* (*Tbp*) (forward: 5′-GAAGCTGCGGTACAATTCCAG-3′; reverse: 5′-CCCCTTGTACCCTTCACCAAT-3′), *adrenoceptor beta 3* (*Adrb3*) (forward: 5′-GGCCCTCTCTAGTTCCCAG-3′; reverse: 5′-TAGC-CATCAAACCTGTTGAGC-3) and *Rap guanine nucleotide exchange factor 3* (*Rapgef3*) (forward: 5′-TCTTACCAGCTAGTGTTCGAGC-3′; and reverse: 5′-AATGCCGATATAGTCGCAGATG - 3′). All the primers were

used at a final concentration of 250 nM. The results were analyzed using $2^{-\Delta\Delta CT}$ relative quantitation.

For immunoblotting, total tissue lysates were prepared in RIPA lysis and extraction buffer (Thermo Fisher Scientific, 89900) containing 1X protease inhibitor (Thermo Fisher Scientific, 78430). Tissue lysates were quantified using DC Protein Assay Reagent (Bio-Rad, 5000111) and denatured at 95 °C for 5 min. To detect the total adiponectin in circulation, plasma samples were prepared by mixing with 4X SDS loading buffer, incubating at 95 °C for 5 min, and cooling on ice. The tissue protein lysates and plasma samples were separated by SDS-PAGE. To separate multimeric complexes of adiponectin, the plasma samples were mixed with non-reducing buffer (10 mM Tris—HCL pH 6.8, 0.6% SDS, 2% glycerol, and 0.01% bromophenol blue) and incubated at room temperature for 20 min before loading to Bis-Tris gradient gels (Thermo Fisher Scientific, NuPAGE 4—12% Midi Protein Gels, WG1402BOX). Antibodies against adiponectin, β-actin, and UCP1 were purchased from Sigma—Aldrich (A6354, A2228, and U6382, respectively). Antibodies against tyrosine hydroxylase and vinculin were purchased from Abcam (ab112 and ab73412, respectively).

2.5. OGTT and ITT

Oral glucose tolerance tests (OGTT) and corresponding insulin measurements were performed by the University of Michigan Metabolism, Bariatric Surgery, and Behavior Core. Briefly, the mice were fasted for 6 h (8:00 am-2:00 pm) and orally gavaged with 60 mg glucose in PBS. A fixed dose of glucose, rather than a dose based on the weight of the mouse, was used to prevent the administration of excess glucose to the Arc$Pomc^{-/-}$ mice because of their obesity relative to the control group as previously discussed [61,62]. Blood was sampled at 0, 15, 30, 60, and 120 min for glucose (Accu-Check glucometer, Roche) and insulin measurements (Millipore rat/mouse insulin ELISA kit, EZRMI-13 K). For insulin tolerance tests (ITT), the animals were fasted for 5 h (9:30 am-2:30 pm) and 1 U kg^{-1} insulin per body weight was injected intraperitoneally. Blood glucose was measured at 0, 15, 30, 60, and 120 min after insulin injection. The HOMA index was calculated using fasting glucose * fasting insulin/22.5.

2.6. Adiponectin, catecholamine, and MSH measurements

Tail blood was collected from a lateral tail vein nick into heparinized glass pipettes and centrifuged at 4 °C for 20 min at 2000 g and plasma adiponectin was assessed using kits from R&D (MRP300 and DY1119) according to the manufacturer's instructions. To measure catecholamines, brown fat, gonadal fat, and subcutaneous fat were homogenized in 0.01 N HCL with EDTA (1 mM) and sodium metabisulfite (4 mM) to prevent catecholamine degradation. The concentration of norepinephrine and epinephrine was measured using an ELISA kit from LDN (BA E—5400) as described by the manufacturer. Plasma MSH levels were measured using an EIA kit from Phoenix Pharmaceuticals (EK-043-01) according to the manufacturer's instructions.

2.7. Statistics

Two-tailed Student's *t*-tests were conducted to determine the significant differences between pairs of genotypes with one dependent variable. One-way or two-way ANOVA followed by Tukey's or Bonferroni's multiple comparison tests were conducted for pair-wise comparisons. A detailed description of the statistical method used for each analysis is noted in each figure legend. $P < 0.05$ was considered significant. Statistical analyses were conducted using GraphPad Prism 8.

3. RESULTS

3.1. Circulating adiponectin increased in the obese *Pomc*-deficient mice

To determine the functional role of POMC neurons in regulating adiponectin, we measured the circulating adiponectin levels in both sexes of the Arc*Pomc*$^{-/-}$ mice at 4 weeks, 8—9 weeks, 16—17, weeks and 47—52 weeks during the development of obesity (Figure 1A,B and Figure 3D). At 4 weeks old, the Arc*Pomc*$^{-/-}$ mice had similar body weights and circulating adiponectin levels in both sexes. At 9 weeks old, the Arc*Pomc*$^{-/-}$ mice had much higher body weights in both males and females compared to the wild-type control mice. A 30%—40% higher level of plasma adiponectin was also detected in both sexes at this age (male: Arc*Pomc*$^{-/-}$: 9.2 ± 0.4 vs *Pomc*$^{+/+}$: 6.6 ± 0.3 μg/mL; female: Arc*Pomc*$^{-/-}$: 11.7 ± 0.3 vs *Pomc*$^{+/+}$: 8.9 ± 0.3 μg/mL) (Figure 1A,B). A similar increase in the circulating adiponectin level was also observed in the female Arc*Pomc*$^{-/-}$ mice with an inbred 129S6/SvEvTac genetic background at the same age (Supplementary Figure 1A). Our previous study monitoring body weights in Arc*Pomc*$^{-/-}$ mice showed that these mice continue gaining weight rapidly until age 13—15 weeks and then reach a plateau [57]. Therefore, we measured the adiponectin levels at 16 weeks and 47—53 weeks when they exhibited their maximum body weights. Unexpectedly, the adiponectin levels in Arc*Pomc*$^{-/-}$ mice at these ages exhibited a sexually dimorphic pattern. A significant increase in adiponectin, compared to control mice, was found in the female Arc*Pomc*$^{-/-}$ mice at 16 weeks of age (Figure 1A) but not in the male

mice (Figure 1B). A 30% increase was found in the female Arc*Pomc*$^{-/-}$ mice aged 48—52 weeks (Figure 3D) but not in the male mice aged 47—50 weeks (Arc*Pomc*$^{-/-}$: 8.7 ± 0.2 vs *Pomc*$^{+/+}$: 8.8 ± 0.6 μg/mL) (Figure 1B). We measured the protein levels of the low-molecular-weight trimers, medium-molecular-weight hexamers, and high-molecular-weight multimers to determine which forms of adiponectin contributed to the increase in the total adiponectin in the Arc*Pomc*$^{-/-}$ mice. Notably, all three forms were significantly increased in the Arc*Pomc*$^{-/-}$ mice (Figure 1C). The full-length form of adiponectin was also significantly elevated, which was consistent with the ELISA detection results as shown in Figure 1A,B.

3.2. Increased adiponectin in the Arc*Pomc*$^{-/-}$ mice was due to the loss of *Pomc* expression in arc

Our previous studies indicated that the increased body weights of Arc*Pomc*$^{-/-}$ mice are due to a significant increase in fat mass [6,55,57]. Therefore, we wondered whether elevated adiponectin was part of the secondary effects of obesity in Arc*Pomc*$^{-/-}$ mice or the result of the loss of *Pomc* expression in Arc independent of fat mass. We conducted a series of calorie-restriction experiments. In the first experiment, we single housed and food restricted 15-week-old female Arc*Pomc*$^{-/-}$ mice for 7 weeks until their body weights were not significantly different from their littermate wild-type controls (Figure 2A). The control mice also underwent a calorie-restriction process to maintain ∼85—90% of their initial pre-treatment body weights. At 15 weeks of age, the Arc*Pomc*$^{-/-}$ mice were significantly heavier than the *Pomc*$^{+/+}$ mice (Figure 2A) mainly due to increased fat
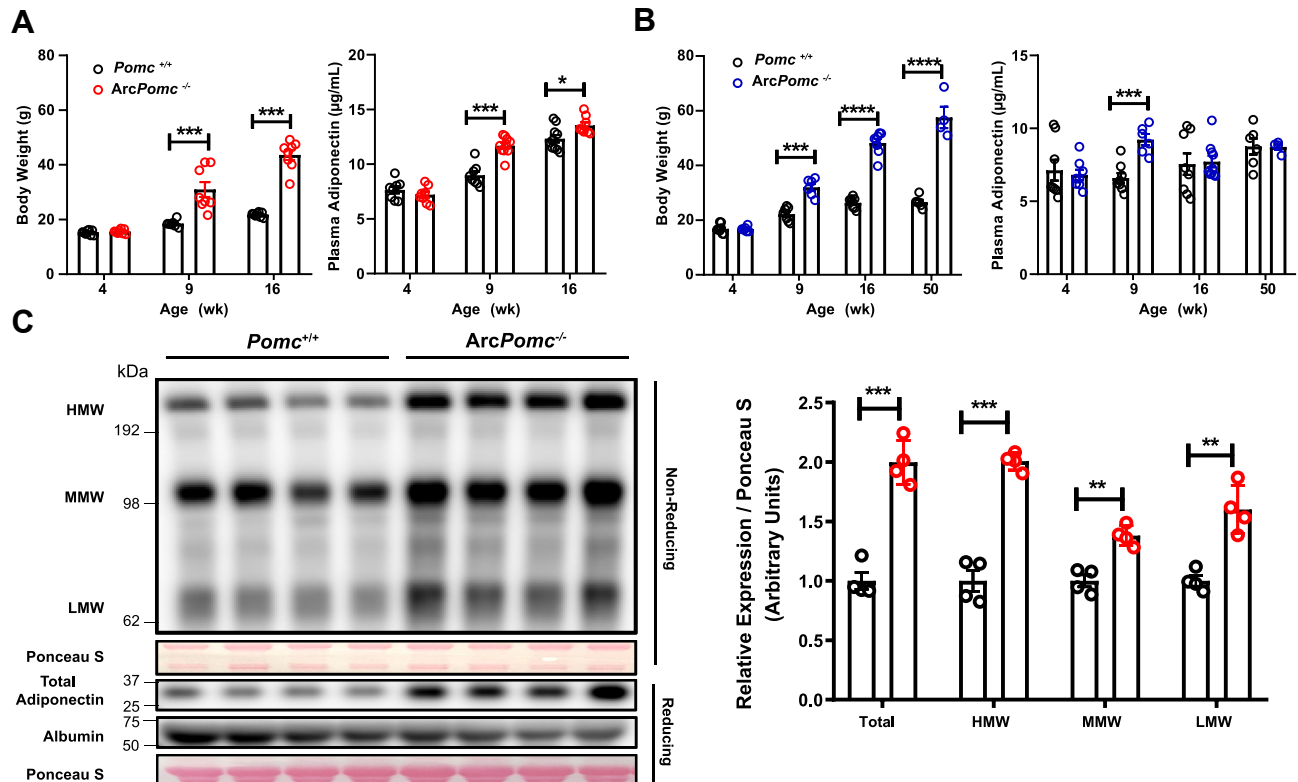

Figure 1: Increased plasma adiponectin in obese hypothalamic *Pomc*-deficient mice. Comparison of body weights and circulating adiponectin levels in *Pomc*$^{+/+}$ and Arc*Pomc*$^{-/-}$ female (A) and male (B) mice on a congenic C57BL/6 J genetic background at the indicated ages (n = 6—10). (C) Immunoblots of plasma protein from 8 to 9-week-old female *Pomc*$^{+/+}$ and Arc*Pomc*$^{-/-}$ mice with a congenic C57BL/6J genetic background. Total, high-molecular-weight (HMW), medium-molecular-weight (MMW), and low-molecular-weight (LMW) adiponectin band intensities were quantified using ImageJ (right) (n = 4). Two-tailed unpaired Student's *t*-tests were used for comparisons. Data shown are the mean ± s.e.m. of biologically independent samples. *$P < 0.05$, **$P < 0.01$, ***$P < 0.001$, and ****$P < 0.0001$.
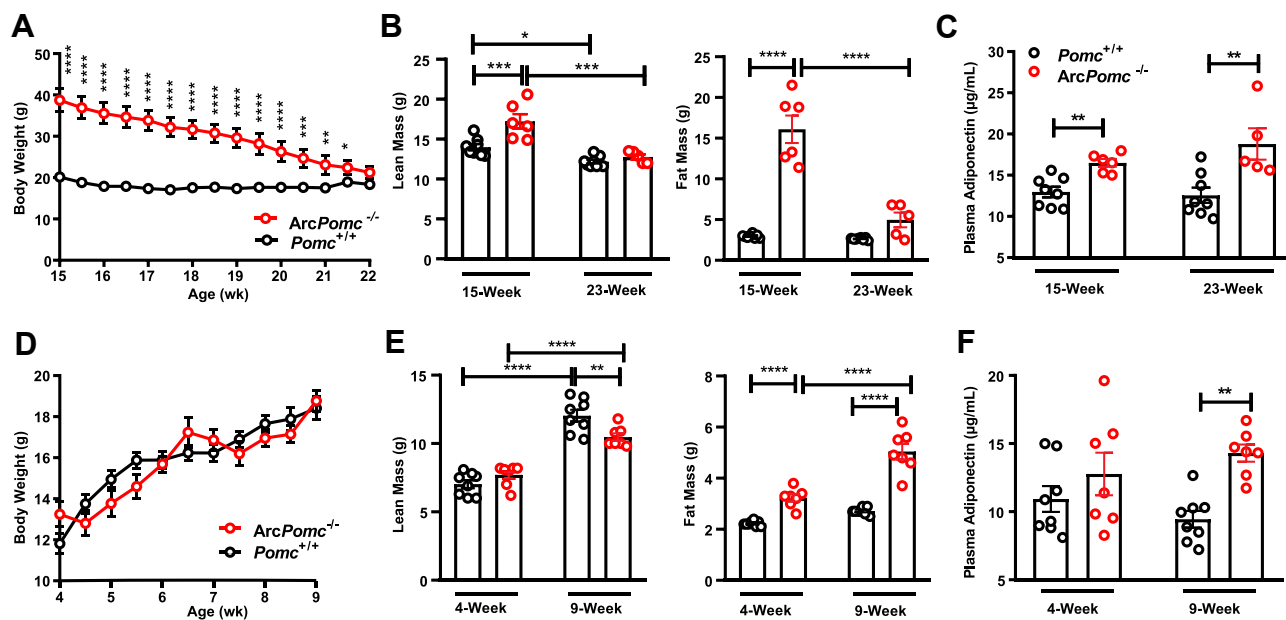
Figure 2: Increased plasma adiponectin in Arc*Pomc*$^{-/-}$ mice was independent of body weight and fat mass. Restricted feeding was performed on 15-week-old female Arc*Pomc*$^{-/-}$ mice for 7 weeks (n = 5−8). Body weights (A), body composition (B), and plasma adiponectin (C) before and after food restriction. Pair-feeding was conducted on 4-week-old female Arc*Pomc*$^{-/-}$ mice for 5 weeks (n = 7−8). Body weights (D), body composition (E), and plasma adiponectin (F) before and after pair-feeding. Two-way ANOVAs or mixed-effects models (depending on the missing values) were used to analyze the effects of treatment and genotype. *Post hoc* Bonferroni's and Tukey's multiple comparisons were conducted. Data shown are the mean ± s.e.m of biologically independent samples. *$P < 0.05$, **$P < 0.01$, ***$P < 0.001$, and ****$P < 0.0001$.

mass (fat mass: Arc*Pomc*$^{-/-}$: 16.1 ± 1.7 vs *Pomc*$^{+/+}$: 3.0 ± 0.1 g) (Figure 2B). Food restriction significantly reduced adiposity by ∼70% in the Arc*Pomc*$^{-/-}$ mice (before: 16.1 ± 1.7 vs after: 5.0 ± 0.9 g), whereas only 10% of adipose tissue decreased in the *Pomc*$^{+/+}$ mice (before: 2.9 ± 0.1 vs 2.6 ± 0.1 g). As expected, the Arc*Pomc*$^{-/-}$ mice had a significantly higher level of adiponectin at 15 weeks old. The decrease in body weight and adiposity did not change this pattern. At 23 weeks old, the Arc*Pomc*$^{-/-}$ mice still exhibited ∼49% more adiponectin compared to the *Pomc*$^{+/+}$ control mice (Figure 2C). We conducted the same experiment using the male mice; however, the Arc*Pomc*$^{-/-}$ male mice had similar adiponectin levels compared to their littermates after calorie restriction (Supplementary Figure 1B), reinforcing that POMC neurons regulate adiponectin levels in a sexually dimorphic pattern.

In the second experiment, we measured plasma adiponectin in weight-matched 9-week-old female mice with no history of being overweight. Following weaning, the Arc*Pomc*$^{-/-}$ mice were fed 75−80% of the average amount of daily food intake of their *Pomc*$^{+/+}$ littermates to maintain equivalent body weights between the two genotypes (Figure 2D). The Arc*Pomc*$^{-/-}$ mice still exhibited significantly increased fat mass (Arc*Pomc*$^{-/-}$: 5.0 ± 0.3 vs *Pomc*$^{+/+}$: 2.7 ± 0.05 g), corresponding to a decrease in lean mass (Arc*Pomc*$^{-/-}$: 10.5 ± 0.3 vs *Pomc*$^{+/+}$: 12.0 ± 0.5 g) at 9 weeks of age (Figure 2E). The female Arc*Pomc*$^{-/-}$ mice had increased tissue weights in their subcutaneous fat, gonadal fat, and brown fat, but not in the liver (Supplementary Figure 1C). Our previous study suggested that *ad libitum* fed female Arc*Pomc*$^{-/-}$ mice at P60 (∼9 weeks) contained approximately 15 g of fat mass [57]. Although restricted feeding did not completely correct the quantity of adiposity from the Arc*Pomc*$^{-/-}$ mice to the same as their *Pomc*$^{+/+}$ siblings, the weight-matched Arc*Pomc*$^{-/-}$ exhibited a substantial reduction in fat mass compared to the *ad libitum* fed animals. At 9 weeks old, the weight-

matched Arc*Pomc*$^{-/-}$ mice had 51% more circulating adiponectin compared to the pair-fed *Pomc*$^{+/+}$ controls (Arc*Pomc*$^{-/-}$: 14.3 ± 0.6 vs *Pomc*$^{+/+}$: 9.4 ± 0.6 µg/mL) (Figure 2F). These results suggest that the increased levels of adiponectin in the *Pomc*-deficient mice were independent of body weight and adiposity.

3.3. Restoration of neuronal *Pomc* expression in the Arc*Pomc*$^{-/-}$ mice decreased their circulating adiponectin

We speculated that the loss of *Pomc* expression in Arc increased adiponectin. To test this hypothesis, we used a conditional Arc*Pomc*$^{-/-}$ transgenic mouse model intercrossed with *Pomc*-CreERT mice. Hypothalamic *Pomc* expression in these compound mice was restored after tamoxifen injection (Figure 3A). The weight of the female *Pomc*-CreERT:Arc*Pomc*$^{-/-}$ mice treated with tamoxifen decreased dramatically from approximately 148% more to only 50% more than the *Pomc*$^{+/+}$ controls (Figure 3B) within 53 days after tamoxifen administration. Notably, 4 weeks post-treatment, the body weights of the *Pomc*-CreERT:Arc*Pomc*$^{-/-}$ mice reached a plateau but remained significantly higher than the *Pomc*-CreERT:Arc*Pomc*$^{+/+}$ control mice (*Pomc*-CreERT:Arc*Pomc*$^{-/-}$: 38.63 ± 2.65 vs *Pomc*-CreERT:Arc*Pomc*$^{+/+}$: 25.7 ± 0.61 g). At 53 days post-tamoxifen injection, the *Pomc*-CreERT:Arc*Pomc*$^{-/-}$ mice still had heavier adipose tissues and livers than the control mice (Figure 3C). These results indicated that restoring *Pomc* expression at a later developmental stage does not fully rescue the obesity phenotype, which is consistent with our previous report [57]. The two-way ANOVA analysis of circulating adiponectin revealed significant effects of tamoxifen treatment, genotype, and their interaction ($F_{treatment}$ (1, 16) = 76.07, $P_{(treatment)} < 0.0001$, $F_{genotypes}$ (2, 16) = 7.714, $P_{(genotypes)} = 0.0045$, $F_{interaction}$ (2, 16) = 4.388, and $P_{(interaction)} = 0.0302$). Specifically, before tamoxifen treatment, the *Pomc*-CreERT:Arc*Pomc*$^{-/-}$ mice had 32% higher adiponectin compared to the *Pomc*-CreERT:Arc*Pomc*$^{+/+}$
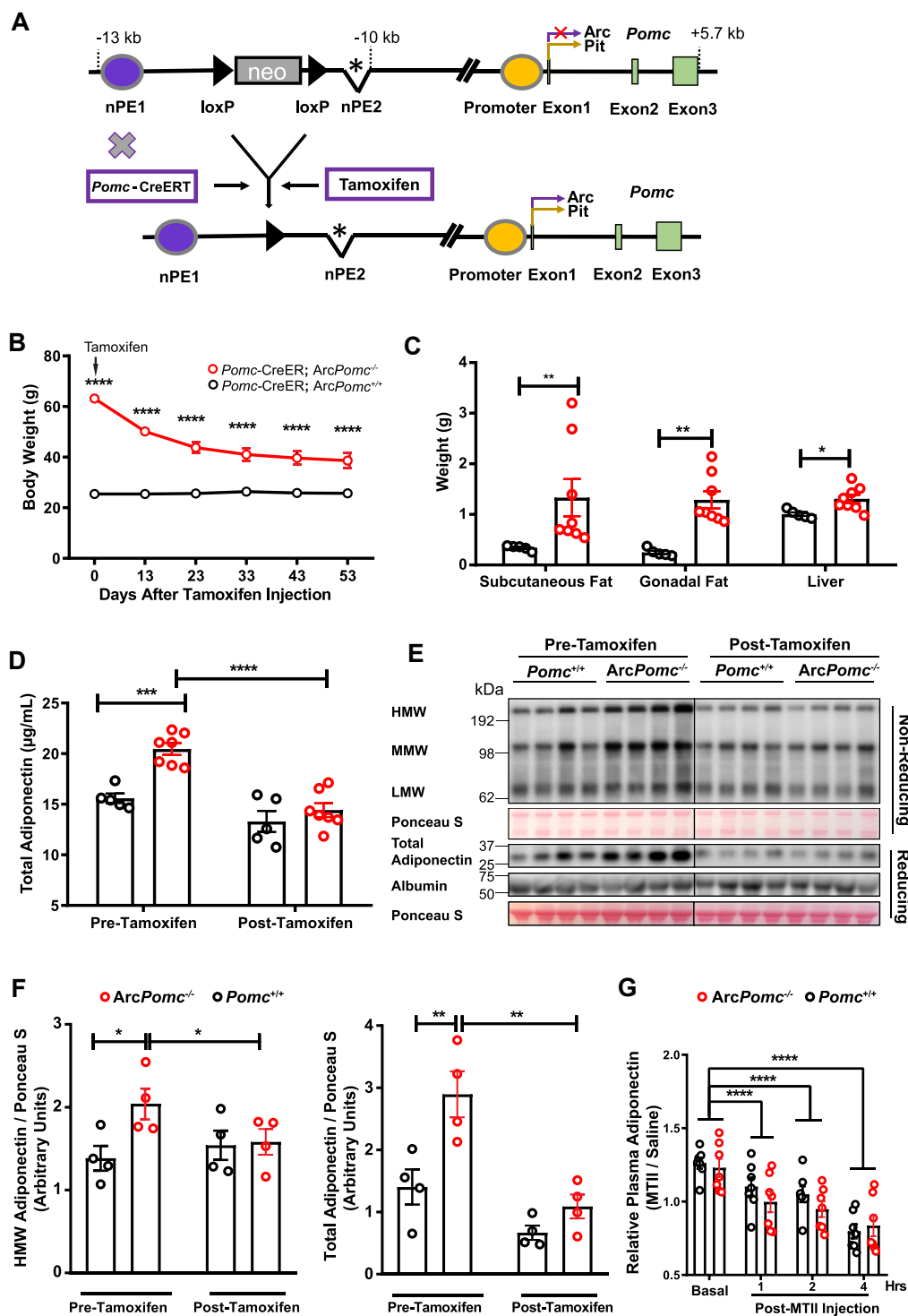
Figure 3: Reactivation of *Pomc* expression in the arcuate nucleus or MTII treatment reduced plasma adiponectin. (A) Schematic representation of the generation of transgenic mice with Cre recombinase-inducible activation of *Pomc* gene expression in the arcuate nucleus after tamoxifen injection. The inducible Arc*Pomc*−/− transgenic mice had a loxP-flanked neomycin (neo) resistance cassette inserted upstream of the deleted neuronal *Pomc* enhancer 2 (nPE2*) in the *Pomc* gene. Purple oval, neuronal *Pomc* enhancer 1 (nPE1); yellow oval, *Pomc* promoter; and green boxes, *Pomc* exons. (B) Serial body weights of 41- to 55-week-old female mice at the indicated time points after tamoxifen injection (n = 5−7). (C) Tissue weight 53 days post-tamoxifen injection (n = 5−7). (D) Plasma adiponectin before and after *Pomc* gene activation in Arc (n = 5−7). (E) Immunoblots of plasma protein from female inducible Arc*Pomc*−/− and Pomc+/+ mice pre- and post-activation of *Pomc* expression in Arc (n = 4). (F) Relative total and high molecular weight adiponectin band intensities (n = 4). (G) Plasma adiponectin levels after melanotan II administration (n = 7, 13−17 weeks old, female). Values were normalized to saline injection within genotypes at respective time points. Two-way ANOVAs with *post hoc* Bonferroni's and Tukey's multiple comparisons were conducted to examine the genotype and tamoxifen treatment effects. Two-tailed unpaired nonparametric Mann−Whitney tests were used for comparisons of tissue weights. Data shown are the mean ± s.e.m of biologically independent samples. *$P < 0.05$, **$P < 0.01$, ***$P < 0.001$, and ****$P < 0.0001$.

controls. Tamoxifen treatment significantly reduced the plasma adiponectin in *Pomc*-CreERT:Arc*Pomc*$^{-/-}$ mice (before: 20.5 ± 0.6 and after: 14.4 ± 0.7 µg/mL). Tamoxifen induction did not significantly change adiponectin levels in the *Pomc*-CreERT:Arc*Pomc*$^{+/+}$ mice (before: 15.6 ± 0.5 and after: 13.3 ± 1.0 µg/mL) (Figure 3D). Electrophoretic separation of plasma proteins for western blotting under non-reducing conditions indicated a significant decrease in the high-molecular weight adiponectin along with a reduction in the total adiponectin (Figure 3E,F). The recovery of *Pomc* expression restores central melanocortin anorectic activity [57]. Therefore, we wondered whether pharmacologically enhanced melanocortin signaling would also lead to reduced circulating adiponectin. We injected MTII (a potent melanocortin receptor agonist) intraperitoneally in obese female Arc*Pomc*$^{-/-}$ and normal weight *Pomc*$^{+/+}$ mice and examined the circulating adiponectin levels. Several studies have shown that MTII treatment can induce a robust reduction in food intake and body weight (primarily from decreased adipose tissue) within 24 h [63,64]. Studies have also suggested that MTII exerts anorectic effects within 4 h [65]. To avoid the confounding metabolic effects of anorexia, we measured the adiponectin levels in a short time period. We fasted the animals continuously for 3 h before treatment and then for the entire 4-hour measuring period. MTII treatment significantly the decreased adiponectin levels across all of the examined time points (Figure 3G). A time-dependent pattern was observed as adiponectin was progressively reduced as the time increased after MTII treatment. The Arc*Pomc*$^{-/-}$ mice responded to MTII injection similarly to the *Pomc*$^{+/+}$ mice. A previous study using intracerebroventricular infusion of SHU9119 (a melanocortin receptor antagonist) reported an increase in circulating adiponectin levels [66], which provides complementary evidence on the modification of central melanocortin signaling to influence peripheral adiponectin levels.

3.4. Reduced sympathetic output to the adipose tissue, but not direct melanocortin signaling in adipocytes, contributed to the increased adiponectin in the ArcPOMC-deficient mice

Adipocytes abundantly express melanocortin 2 receptor (*Mc2r*) and melanocortin 5 receptor (*Mc5r*) [67]. Because MTII possesses partial agonist functional efficacy at mouse MC5R [68] and mouse MC2R responds to ACTH stimulation with high binding affinity to ACTH [69,70], we examined whether MTII and ACTH could directly affect adiponectin secretion from adipocytes *in vitro*. We treated mature adipocytes with MTII and ACTH at the indicated doses and examined the adiponectin levels in the culture medium at several time points. Two-way ANOVA showed that neither of these drugs induced any dose-dependent changes in adiponectin levels (Supplementary Figure 2A and B), MTII: F (3, 20) = 1.646, *P* = 0.2105, ACTH: F (3, 20) = 2.36, *P* = 0.1021). Under basal conditions, the Arc*Pomc*$^{-/-}$ mice had similar plasma ACTH levels [71] and α-MSH levels as the *Pomc*$^{+/+}$ control mice (Supplementary Figure 2C), suggesting that the increased adiponectin in the Arc*Pomc*$^{-/-}$ mice was unlikely caused by changes in circulating melanocortin peptides secreted from the pituitary gland.

Next, we wondered how the restoration and activation of the central melanocortin system affects adipose tissue to increase circulating adiponectin levels if it is not due to direct melanocortin signaling in adipocytes. Several lines of evidence suggested that the central melanocortin system can affect adipose tissue by altering the activity of sympathetic nerves that innervate adipose tissue [19,72—74]. Exposing the Arc*Pomc*$^{-/-}$ mice to a decreased environmental temperature of 4 °C rapidly reduced their core body temperatures from an average of 37.2 °C—27.1 °C within 4 h, while the *Pomc*$^{+/+}$ mice

exhibited only a small decrease in body temperature (Figure 4A). The thermogenic defects in the Arc*Pomc*$^{-/-}$ mice indicated that reduced sympathetic outflow or impaired adrenergic signaling may have occurred in their thermogenic fat. Therefore, we measured the epinephrine and norepinephrine (the major types of catecholamines that are essential for thermogenesis) concentrations in their intrascapular brown, subcutaneous, and gonadal fat depots. The results revealed that the female Arc*Pomc*$^{-/-}$ mice had significantly lower levels of both epinephrine and norepinephrine in all three of the examined fat tissues compared to the *Pomc*$^{+/+}$ controls (Figure 4B). Nearly identical genotype differences were found in the male mice cohorts (Supplementary Figure 3). The striking reduction in the catecholamine concentrations in the Arc*Pomc*$^{-/-}$ adipose tissues raised the possibility of a reduction in sympathetic innervation in these tissues. Therefore, we measured the protein levels of tyrosine hydroxylase (TH), a rate-limiting enzyme in catecholamine biosynthesis that is a marker of sympathetic nerve fibers in brown fat and subcutaneous fat. There was a significant reduction in the TH protein levels in the brown fat from both the males and females (Figure 4C). We also measured a significant decrease in the UCP1 protein levels, which may have partially accounted for the cold intolerance in the Arc*Pomc*$^{-/-}$ mice. A similar reduction in TH was also observed in the subcutaneous fat in the female mice; however, a small decrease in TH in the subcutaneous fat in the male Arc*Pomc*$^{-/-}$ mice was not statistically significant different from the *Pomc*$^{+/+}$ males.

We treated the female Arc*Pomc*$^{-/-}$ mice with norepinephrine to pharmacologically mimic the effects of increased sympathetic activation on adiponectin secretion from the adipocytes. Consistent with the previously presented data, the circulating adiponectin significantly decreased from baseline levels 4 h after treatment (1.7-fold decrease, Figure 4D). In contrast, the beta-adrenergic antagonist propranolol significantly increased the circulating adiponectin (Figure 4E). The *Pomc*$^{+/+}$ mice also responded to norepinephrine and propranolol treatments with a similar pattern to the Arc*Pomc*$^{-/-}$ mice (data not shown). These results were consistent with a previous report, which indicated that cold exposure suppressed serum adiponectin whereas inhibition of the sympathetic nervous system restored adiponectin levels [75—77].

3.5. Increased plasma adiponectin was derived mainly from subcutaneous adipose tissue

To follow up our finding of reduced sympathetic outflow to brown, subcutaneous, and gonadal fat (Figure 4), we examined which fat depot was the major contributor to the increased plasma adiponectin in the female mice, focusing on subcutaneous and gonadal fat depots because of their relatively high total mass. We first compared the adiponectin protein levels in these two tissues between the Arc*Pomc*$^{-/-}$ and *Pomc*$^{+/+}$ mice. Subcutaneous but not gonadal fat from the Arc*Pomc*$^{-/-}$ mice exhibited increased levels of adiponectin (Figure 5A). In line with the protein levels, the adiponectin mRNA abundance was 2.7-fold higher in the subcutaneous fat of the Arc*Pomc*$^{-/-}$ compared to the *Pomc*$^{+/+}$ mice, but there were no genotype differences in either gonadal or brown fat depots (Figure 5B). A previous study showed that blunted adiponectin secretion in obese/type 2 diabetic mice was partially due to the reduced transcript abundance of *Rap guanine nucleotide exchange factor 3* (*Rapgef3*) and *adrenoceptor beta 3* (*Adrb3*) in primary subcutaneous adipocytes [78]. We therefore examined *Rapgef3* and *Adrb3* gene expression in both the subcutaneous and gonadal fat tissue of the rats in the current study. Compared to the *Pomc*$^{+/+}$ mice, the Arc*Pomc*$^{-/-}$ mice had significantly increased steady-state mRNA levels of both *Rapgef3* and
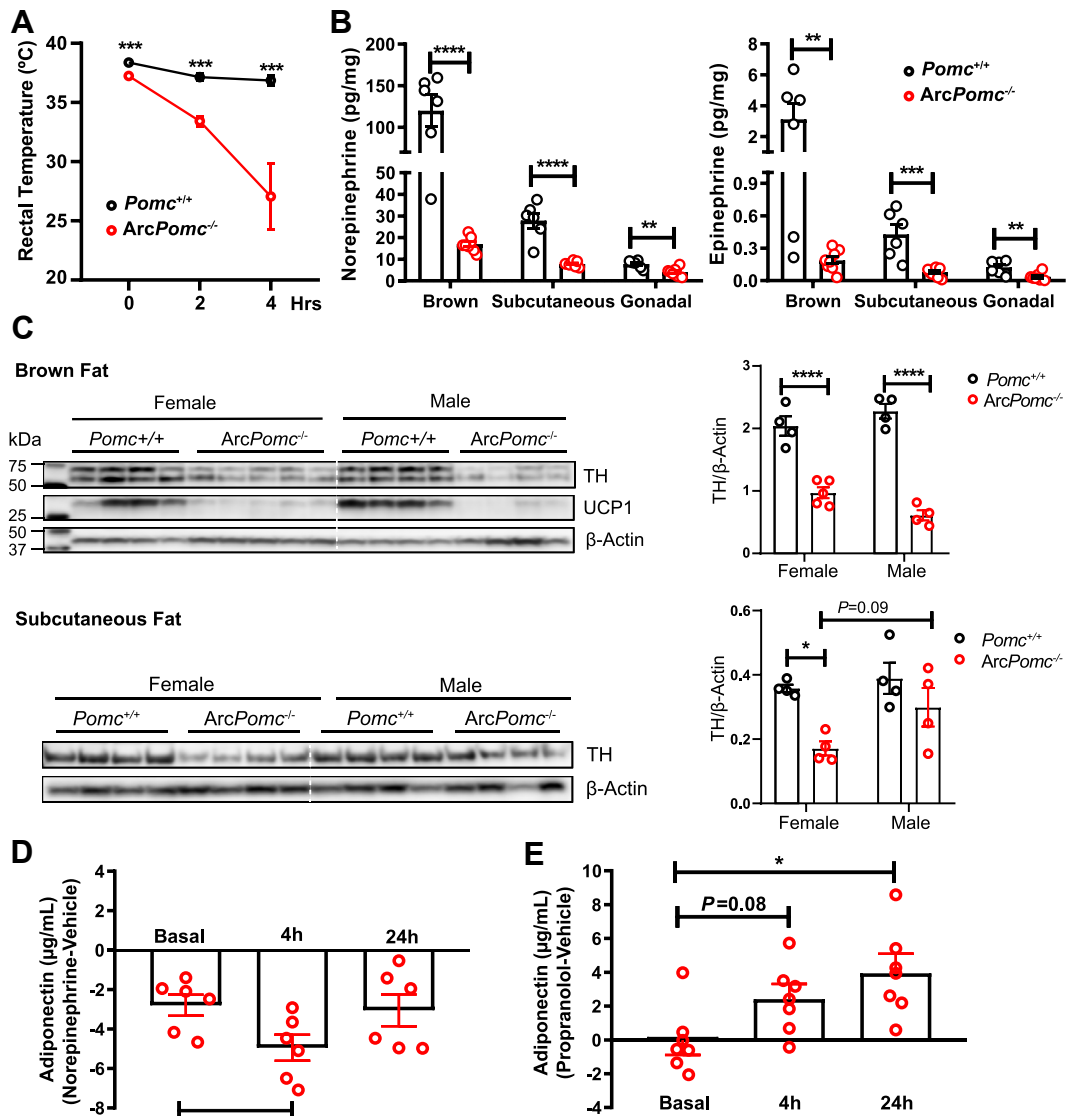
Figure 4: Reduced central sympathetic outflow to adipose tissue contributed to the elevated level of plasma adiponectin in the Arc*Pomc*$^{-/-}$ mice. (A) Changes in rectal temperature during 4 h of cold exposure (4 °C) (n = 5, female mice, 30 weeks old). (B) Measurement of catecholamine concentrations in adipose tissue (n = 6–8, female mice, 24–30 weeks old). (C) Immunoblots of total brown fat and subcutaneous fat lysates from *Pomc*$^{+/+}$ and Arc*Pomc*$^{-/-}$ mice (n = 4–5). Relative tyrosine hydroxylase (TH) band intensity was quantified using ImageJ (right). (D) Plasma adiponectin levels of Arc*Pomc*$^{-/-}$ mice in response to norepinephrine treatment. Within-subject post-vehicle treatment values were subtracted from the post-norepinephrine treatment values (n = 6–7, female mice, 15–21 weeks old). (E) Plasma adiponectin levels of the Arc*Pomc*$^{-/-}$ mice in response to propranolol treatment. Within-subject post-vehicle treatment values were subtracted from the post-propranolol treatment values (n = 6–7, female mice, 20–25 weeks old). Two-tailed unpaired Student's *t*-tests were used to compare changes in body temperature, catecholamine concentrations, and norepinephrine/propranolol treatment effects. *Post hoc* Bonferroni's multiple comparisons following two-way ANOVAs were used to examine the genotype and sex effects on TH protein quantification. Data shown are the mean ± s.e.m of biologically independent samples. *$P < 0.05$, **$P < 0.01$, ***$P < 0.001$, and ****$P < 0.0001$.

Adrb3 in their subcutaneous fat (Figure 5C,D). In contrast, there was no genotype difference in *Rapgef3* expression but a markedly decreased expression of *Adrb3* in the gonadal fat of the female Arc*Pomc*$^{-/-}$ mice compared to the *Pomc*$^{+/+}$ mice. These data together suggest that subcutaneous fat was the main contributor to the increased plasma adiponectin in the Arc*Pomc*$^{-/-}$ mice.

3.6. Deletion of adiponectin in the Arc*Pomc*$^{-/-}$ mice did not change their growth curves, obesity phenotypes, or glucose homeostasis

To examine whether increased circulating adiponectin in the female Arc*Pomc*$^{-/-}$ mice mitigated their metabolic dysfunction, we introduced adiponectin-null mice (*Adipoq*$^{-/-}$) from the Jackson Laboratory to our breeding method to generate animals lacking both adiponectin and Arc*Pomc* expression (Arc*Pomc*$^{-/-}$:*Adipoq*$^{-/-}$). Overexpression of adiponectin in *ob/ob* mice actually leads to increased body weight and fat mass specifically in subcutaneous fat depots [44]. Therefore, we monitored the body weights and compared these and several other metabolic parameters among monogenic the Arc*Pomc*$^{-/-}$ or *Adipoq*$^{-/-}$ mice and compound Arc*Pomc*$^{-/-}$:*Adipoq*$^{-/-}$ mice (Figure 6). Body weights were measured twice a week from 4 weeks to 24 weeks. Deficiency in *Pomc* expression in Arc markedly increased body weights of the mice from 6 weeks old; however, the monogenic lack of adiponectin (*Pomc*$^{+/+}$:*Adipoq*$^{-/-}$) or in
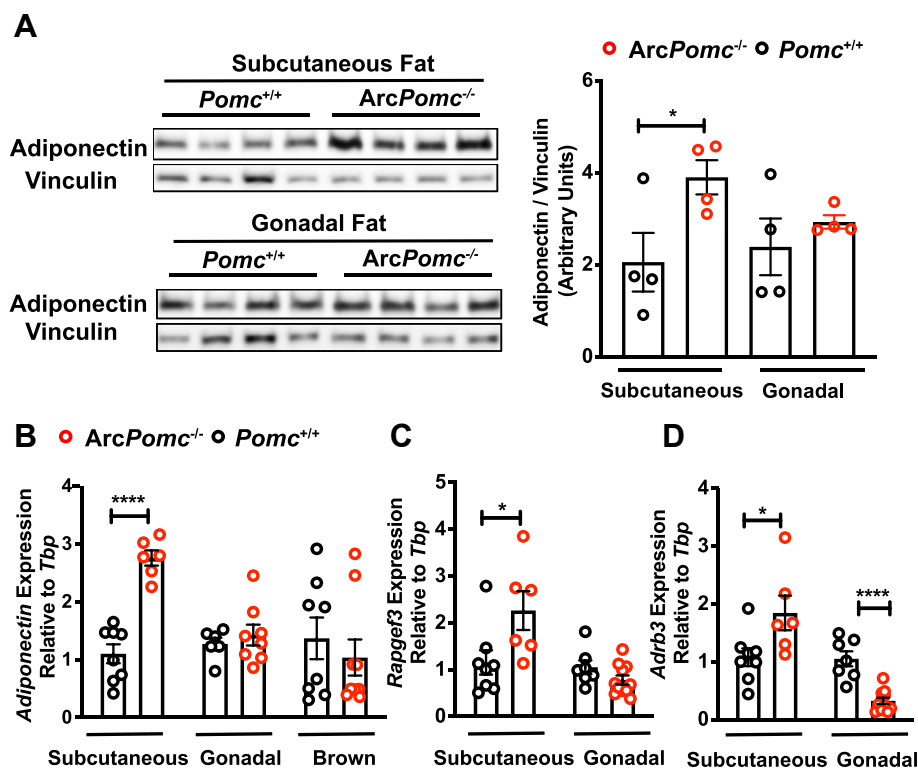
Figure 5: Subcutaneous fat was the primary source of elevated plasma adiponectin in the Arc*Pomc*$^{-/-}$ mice. (A) Immunoblots of total subcutaneous and gonadal fat lysates from 26-week-old female mice (left). Adiponectin band intensity was normalized to vinculin (right) (n = 4). (B) Quantitative PCR analysis of adiponectin mRNA expression in the subcutaneous, gonadal, and intrascapular brown fat (n = 6−8, 8−9 weeks old, female). Quantitative PCR analysis of *Rapgef3* (C) and *Adrb3* (D) in the subcutaneous and gonadal fat (n = 6−8, 8−9 weeks old, female). Two-tailed unpaired Student's *t*-tests were used to compare the genotype effects. Data shown are the mean ± s.e.m of biologically independent samples. *$P < 0.05$, ***$P < 0.001$, and ****$P < 0.0001$.

combination with central *Pomc* deficiency (Arc*Pomc*$^{-/-}$:*Adipoq*$^{-/-}$) had no effect on the growth curves compared to the *Pomc*$^{+/+}$ or Arc*Pomc*$^{-/-}$ mice, respectively, in both sexes (Figure 6A,E). Similarly, the absence of adiponectin did not change the body composition, liver weight, or fat depot weights compared to the monogenic Arc*Pomc*$^{-/-}$ mice. (Figure 6B,C, F, and G). Previous electrophysiological studies highlighted that adiponectin functions directly on POMC neurons in the Arc to regulate food intake [79,80]. Therefore, we also compared the 24-hour food intake among the four genotypes of mice. Adiponectin deficiency in the compound Arc*Pomc*$^{-/-}$:*Adipoq*$^{-/-}$ mutant mice had no significant effect on the food intake of either sex compared to their respective hyperphagic Arc*Pomc*$^{-/-}$:*Adipoq*$^{+/+}$ counterparts (Figure 6D,H).

Although adiponectin has anti-diabetic effects, the obese Arc*Pomc*$^{-/-}$ mice without adiponectin had similarly impaired glucose tolerance and insulin sensitivity as the Arc*Pomc*$^{-/-}$ mice with adiponectin in both sexes (Figure 6I, K, N, and P). Furthermore, the compound Arc*Pomc*$^{-/-}$:*Adipoq*$^{-/-}$ mice had the same elevated fasted plasma insulin levels and insulin dynamics in response to an oral glucose load as the monogenic Arc*Pomc*$^{-/-}$ mice, indicating similar islet function between the two genotypes (Figure 6J and O), which was verified by the unchanged homeostatic model assessment of insulin resistance (HOMA-IR) (Figure 6L and Q). Finally, the 2-hour and 4-hour post-prandial glucose levels following a 16-hour fast were also determined, and again deletion of adiponectin did not induce any significant differences compared to the mice of either sex with only a deficiency in the central *Pomc* expression (Figure 6 M and R).

4. DISCUSSION

It has been clearly established that central POMC deficiency in humans, dogs, and mice leads to hyperphagia and morbid obesity. Maximal *Pomc* expression in the arcuate nucleus requires two phylogenetically conserved enhancers, nPE1 and nPE2. Arc*Pomc*$^{-/-}$ mice with a deletion of both enhancers and the insertion of a loxP-flanked neomycin selection cassette between the two enhancers exhibited greatly reduced *Pomc* expression to ∼1% of wild-type levels in the hypothalamus and subsequently became obese with extremely high fat mass [6]. Obesity and increased fat mass are usually associated with hyperleptinemia but decreased circulating adiponectin. However, the current study showed that obese hyperleptinemic mice with central *Pomc* deficiency exhibited paradoxically elevated levels of plasma adiponectin in an age-dependent and sexually dimorphic manner. The female Arc*Pomc*$^{-/-}$ mice had increased adiponectin at all examined ages, whereas the males only exhibited this phenotype in early adulthood (8−9 weeks old). Weight reduction by calorie restriction showed that increased circulating adiponectin in the female Arc*Pomc*$^{-/-}$ mice was not simply a result of excess fat mass. Remarkably, both genetic activation of the central melanocortin system and pharmacologic stimulation of adrenoreceptors reduced adiponectin levels in the Arc*Pomc*$^{-/-}$ mice, while exposure of adipocytes directly to melanocortin agonists *in vitro* had no effect on adiponectin secretion, indicating that a central regulatory mechanism for adiponectin production and/or secretion was altered in the Arc*Pomc*$^{-/-}$ mice. The melanocortin system can impact adipose tissue indirectly via
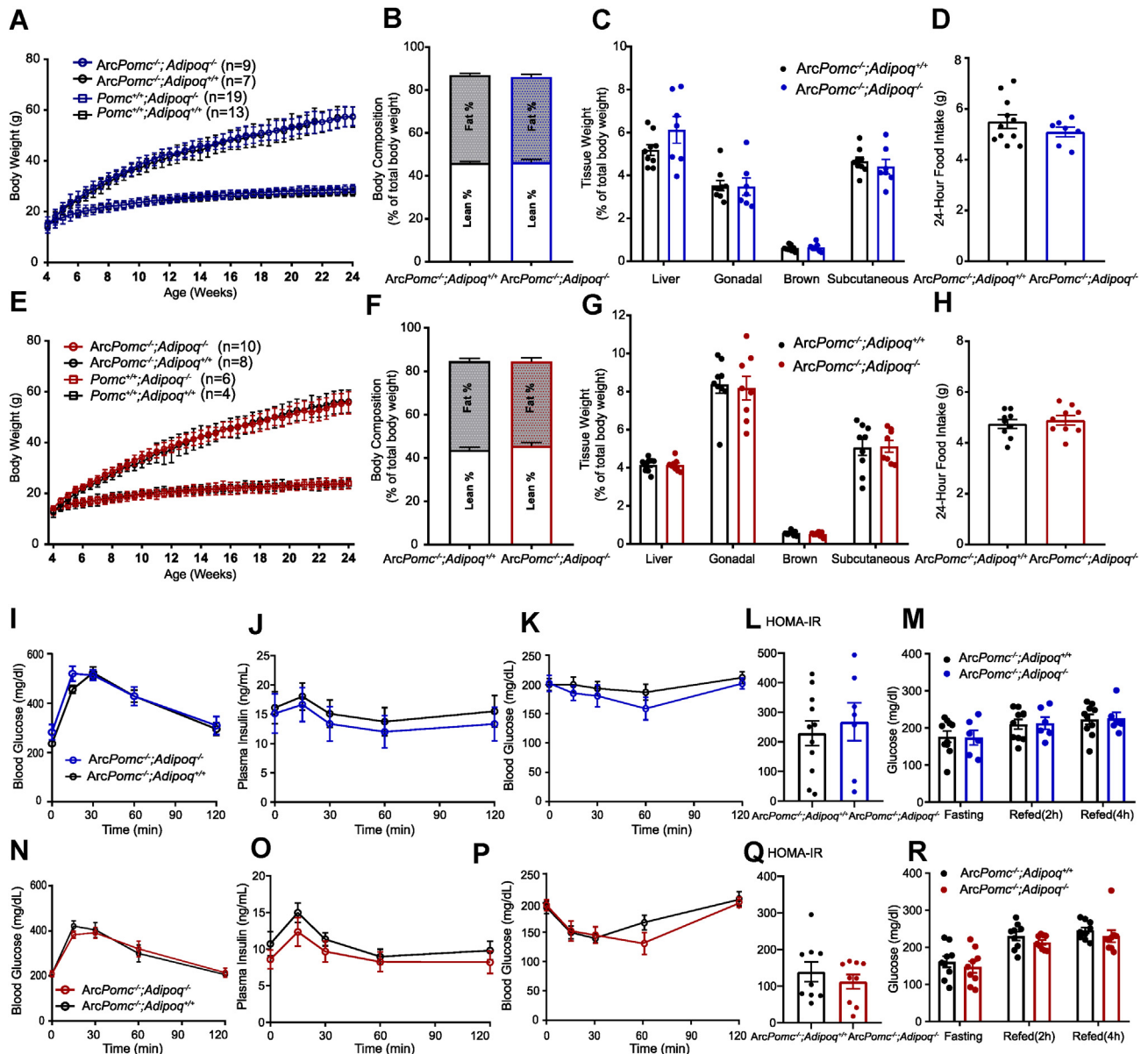
Figure 6: Deletion of adiponectin from the Arc*Pomc*$^{-/-}$ mice had no effect on their metabolic abnormalities. Body weight comparisons of the male (A) and female (E) mice from 4 weeks to 24 weeks of age. Comparisons of the body composition (B: male and F: female) tissue weights (C: male and G: female) and 24-hour food intake (D: male and H: female) between the Arc*Pomc*$^{-/-}$:*Adipoq*$^{+/+}$ and Arc*Pomc*$^{-/-}$:*Adipoq*$^{-/-}$ mice (male, n = 7−11, female, n = 9). (I, J, N, and O) Oral glucose tolerance tests (I: male and N: female) and plasma insulin levels collected at corresponding time points (J: male and O: female). Insulin tolerance tests (K: male and P: female) and HOMA-IR (L: male and Q: female) from the Arc*Pomc*$^{-/-}$:*Adipoq*$^{+/+}$ and Arc*Pomc*$^{-/-}$:*Adipoq*$^{-/-}$ mice (male: n = 6−11 and female: n = 9). Glucose levels from 16-hour fasted, 2-h refed, and 4-h refed mice (M, male: n = 6−10, R, female: n = 9). Two-tailed unpaired Student's *t*-tests were used to compare genotype effects in body composition, tissue weights, 24-hour food intake, HOMA-IR, fasting, and refed glucose levels. Males: 17−22 weeks old; females: 8−12 weeks old.

altering the activity of sympathetic nerves that innervate it. A defective response to acute cold exposure, dramatic reduction in the levels of catecholamines, and markedly lower protein levels of tyrosine hydroxylase in both brown and subcutaneous fat were observed in the Arc*Pomc*$^{-/-}$ animals, implying that deficits in sympathetic nervous outflow to these thermogenic adipose tissues most likely contribute to increased circulating adiponectin.

The current study indicated a physiological role of the central melanocortin system in regulating peripheral adiponectin levels. Melanocortin peptides are derived from post-translational processing of POMC

prohormone and their specific effects are mediated by agonism of a family of melanocortin receptors [81]. Among the five identified receptors, MC3R and MC4R are the two receptors principally expressed in the central nervous system. However, α-MSH has higher affinity binding to MC4R and this receptor is primarily responsible for the melanocortin inhibition of food intake, stimulation of energy expenditure, and reduction in adiposity [67]. MC4R-null mice are hyperphagic and morbidly obese, similar to the phenotype of Arc*Pomc*$^{-/-}$ mice. Although MC4R-null mice exhibit defects in UCP1 expression, they are cold-tolerant without a marked drop in their core body temperature

[18,82], whereas Arc*Pomc*$^{-/-}$ mice are cold-intolerant and will die of hypothermia in long-term low-temperature environment. Because cold-induced thermogenesis is mainly mediated by brown adipose tissue via regulation from the sympathetic nervous system, it is very likely that the deficiency in *Pomc* expression in the Arc results in even less sympathetic drive to brown fat and subcutaneous fat compared to MC4R deficiency. Moreover, the regulation of plasma adiponectin by MC3R cannot be overlooked. Partial inactivation of MC3R with compound C17A and G241A sequence mutations is associated with early onset obesity in children [83]. Interestingly, despite increased fat mass, the circulating adiponectin levels in children with these mutations are significantly higher compared to non-overweight children. This observation was further confirmed in a knock-in mouse model that mimicked human MC3R sequence variants [84]. Furthermore, obese patients with Prader—Willi syndrome (PWS) also have higher levels of circulating adiponectin than those with simple obesity [85]. PWS patients exhibit several clinical features including hyperphagia and obesity. Animal experiments have shown that impaired POMC neuronal function is involved in the development of PWS as evidenced by reduced *Pomc* gene expression, lower POMC neuronal sensitivity to leptin, and decreased post-translational processing of POMC pro-hormone [86—88]. Overall, prior research, together with our study, indicate that deficits in the central melanocortin system can modulate peripheral adiponectin levels. Changes in sympathetic outflow are contributors; however, at this point, we cannot exclude the presence of other unidentified regulatory mechanisms to this phenotype.

Unlike leptin homeostasis in adipocytes, pre-adiponectin is translocated from cytoplasmic ribosomes into the lumen of the endoplasmic reticulum by co-translational proteolytic cleavage of its signal sequence. Subsequently, adiponectin is sorted into secretory vesicles for storage. Vesicle exocytosis is stimulated by increased intracellular concentrations of cAMP, Ca^{++}, and likely additional intracellular second messengers. Catecholamines released from sympathetic neuronal synapses adjacent to the adipocytes bind to and activate different subtypes of adrenergic receptors that regulate intracellular cAMP. Whether the sympathetic tone ultimately increases or decreases circulating adiponectin appears to depend on a balance of many factors including the specific type of fat depot, the density of post-ganglionic sympathetic fibers within a depot, the density and combination of adrenoreceptor subtypes, the rate of clearance of catecholamines from the synaptic cleft, and the duration of sympathetic stimulation [78,89,90]. Most published data from *in vivo* experiments suggest that an elevated sympathetic tone is typically associated with decreased circulating plasma adiponectin [75—77]. Our data are consistent with this relationship because the female Arc*Pomc*$^{-/-}$ mice exhibited a chronic reduction in sympathetic tone in combination with chronic elevations of circulating adiponectin and increased fat content of both *Adipoq* mRNA and adiponectin protein. These features are reversed by genetic restoration of central *Pomc* expression and mimicked by pharmacological treatment with either MTII or norepinephrine.

It is worth noting that in contrast to diet-induced obese models characterized by decreased circulating adiponectin, the obese *Pomc*-deficient mice in the current report had increased mRNA levels of *Rapgef3* and *Adrb3* in their subcutaneous fat depots. An earlier study based on *ex vivo* analyses of isolated adipocytes proposed that adiponectin vesicle exocytosis is acutely stimulated through the activation of *Adrb3* and *Rapgef3* [78]; therefore, the obesity-induced perturbation of adiponectin may result from reduced expression of *Rapgef3* and *Adrb3*. Our finding of a differential expression pattern of increased *Rapgef3* and *Adrb3* in subcutaneous fat but decreased

levels in gonadal fat from the Arc*Pomc*$^{-/-}$ mice may indicate that the systematic changes in *Pomc* deficiency induced obesity are intrinsically different from high-fat diet-induced obesity. Another example is that the obese Arc*Pomc*$^{-/-}$ mice exhibited improved glucose tolerance associated with decreased renal sympathetic tone compared to their *Pomc*$^{+/+}$ littermates [61,62] or diet-induced obese mice.

Other than the current work, little attention has been paid to the role of POMC neurons in regulating circulating adipokines. A recent study by Joel Elmquist's group uncovered an unexpected role of leptin receptor-expressing POMC neurons in regulating fasting-induced decreases in circulating leptin. They showed that mice with leptin receptor deletion specifically from POMC neurons did not have reduced leptin levels during fasting. They demonstrated that this unexpected dynamic change in leptin was independent of adiposity and specific to the visceral adipose tissue [20]. Mechanistically, an increased transcriptional level of *adrenergic receptor a-2a* in the visceral fat was responsible. Taken together, we conclude that central POMC neurons play an essential role in regulating circulating adipokines independent of fat mass, which adds another layer to the complexity of brain-adipose tissue crosstalk. It would be relevant to explore whether POMC neurons regulate the circulating levels of other adipokines, for example, resistin, visfatin, and omentin.

In this study, only the adult female Arc*Pomc*$^{-/-}$ mice continuously exhibited increased adiponectin. Sexually dimorphic adiponectin levels have been previously recognized in both rodents and humans. Our results also indicated an increase in adiponectin in the females compared to the age-matched males, consistent with previous reports [23,24]. Estrogen plays important roles in the central regulation of energy homeostasis and adipose tissue biology. It has direct effects on *Pomc* neurons through estrogen receptor α (Esr1) signaling [91]. Studies showed that ∼30% of *Pomc* neurons express Esr1 [92,93]. Moreover, female mice lacking Esr1 selectively from *Pomc* neurons developed hyperphagia and modest obesity [93]. Accordingly, administration of 17α-estradiol, a non-feminizing isomer of 17α-estradiol, reduced energy intake and decreased fat mass in wild-type high-fat diet-induced obese mice but not in obese hypothalamic *Pomc*-deficient mice [94], indicating that hypothalamic *Pomc* neurons mediated the anorectic effects of 17α-estradiol. Despite its impact on whole body metabolism, estrogen has minimal effects on circulating adiponectin levels since neither ovariectomy nor estrogen replacement changes plasma adiponectin levels in females [24,95]. However, testosterone was determined as one of the factors that reduces adiponectin levels in males since castration increases adiponectin whereas the addition of testosterone reduces both circulating adiponectin and adiponectin secretion from cell cultures [95]. Therefore, we speculated that the male Arc*Pomc*$^{-/-}$ mice may have had increased testosterone levels, which repressed adiponectin secretion from adipose tissue and resulted in equal levels compared with the *Pomc*$^{+/+}$ male mice. We assessed the testosterone levels in 24—28-week-old obese male Arc*Pomc*$^{-/-}$ mice and normal weight *Pomc*$^{+/+}$ control males but did not observe a statistically significant difference between the two genotypes (Arc*Pomc*$^{-/-}$: 1.2 ± 0.4 vs *Pomc*$^{+/+}$: 0.8 ± 0.3 ng/mL).

Another speculation on the mechanisms underlying the sexual dimorphism in adiponectin levels concerns intrinsic sex differences in POMC neurons. A recent study showed that female mice have more POMC neurons, higher *Pomc* transcript abundance, and elevated POMC neural activity than males. However, this sex difference was not found in other Arc neuron types including the AgRP neurons [96]. Our group has reported that reactivation of POMC neurons completely

normalized the food intake of female mice regardless of treatment age, whereas males still exhibited significant residual hyperphagia in adulthood [57]. Using the same *Pomc* reactivatable mice, Heisler's group showed that restoration of *Pomc* expression specifically in 5-hydroxytryptamine 2c receptor expressing neurons normalized physical activity, brown fat lipid accumulation, and expression of important genes associated with thermogenesis (*Pgc-1α* and *Elolv3*) only in male mice [97]. *Pgc-1α* is one of the genes that was originally identified to respond to sympathetic stimulation in brown fat [98]; hence, the lack of induction of *Pgc-1α* together with higher lipid accumulation may indicate lower basal sympathetic activity in female mice compared to male mice. In fact, the sex difference in sympathetic tone has been widely discussed since epidemiological studies revealed that the incidence and severity of hypertension is lower in women than in men. A major corollary finding from these studies is that females have an attenuated response to sympathetic stimulation [99,100].

In one of the experiments in this study, central *Pomc* expression was restored using an inducible CreERT/loxP transgenic system. Tamoxifen was administrated to activate Cre recombinase, which in turn removed the neomycin cassette and restored *Pomc* expression. However, several lines of evidence have shown that tamoxifen impacts adipose tissue metabolism. Tamoxifen can induce immediate adipocyte autophagy, apoptosis, and regeneration [101,102]. The acute death of adipocytes leads to a marked reduction in adiposity and body weight within the first week, which recovers from the second week after tamoxifen administration. Another immediate effect of tamoxifen, even at a low dose, is to promote browning of adipose tissues, including both gonadal fat and subcutaneous fat [103,104]. In those studies, tamoxifen not only remodeled adipose tissue, but also changed whole body glucose and lipid metabolism. Higher serum triglyceride, free fatty acid, and HbA1c were detected 6 weeks after tamoxifen treatment [104]. Intriguingly, tamoxifen remained active and its residuals were still detectable 2 months post-treatment [101]. Although the current study did not closely monitor body composition every week after tamoxifen treatment, a previous study using the same dose of tamoxifen suggested that mice treated with tamoxifen have equivalent body weight and fat mass to naïve controls beginning from 4 weeks post-treatment [102]. A parallel study compared mice with a lower fixed tamoxifen dose and mice with vehicle injection and showed similar body weights and subcutaneous fat and gonadal fat tissue weights; however, the overall percentage of body fat was significantly increased with tamoxifen 6 weeks post-treatment. Regardless, the circulating adiponectin level did not significantly change [104], suggesting that the modulation of adipose tissue by tamoxifen (mainly within the first week) may not have a significant impact on the circulating adiponectin level 6 weeks post-treatment despite the remaining tamoxifen activity. The current study examined adiponectin levels 53 days (∼7 weeks) post-tamoxifen. Considering the aforementioned studies, we do not believe that any tamoxifen residual activity would dramatically change adiponectin levels. More importantly, our control group was also treated with the same dose of tamoxifen and our other experiments that did not involve tamoxifen were all consistent regarding the role of the central melanocortin system on circulating adiponectin.

Although the half-life of adiponectin is short, mice usually maintain stable and abundant levels (>5 ng/mL) in their circulation without marked fluctuations [31]. The consistently ∼30%—40% higher level of adiponectin in female Arc*Pomc*$^{-/-}$ mice over their entire lifetime may therefore have important physiological consequences. Many studies have shown that injection of high doses of recombinant adiponectin significantly lowered serum glucose levels in both wild-type and diabetic mouse models [46,105]. Overexpression of adiponectin in *ob/ob* mice led to significantly elevated body weights with highly increased subcutaneous fat mass compared to *ob/ob* mice, yet they showed improved metabolic phenotypes including better insulin sensitivity and glucose tolerance [44]. Therefore, we crossed Arc*Pomc*$^{-/-}$ mice with adiponectin-null mice to determine whether elevated adiponectin mitigates the severity of metabolic deficits caused by the loss of melanocortin signaling in the brain. Unexpectedly, the absence of adiponectin in the Arc*Pomc*$^{-/-}$ mice did not result in any metabolic improvements in terms of overall growth, body composition, food intake, insulin sensitivity, or glucose homeostasis in either sex. The group that generated the adiponectin-null mice that were used in this study previously showed no significant glucose intolerance or insulin resistance in the mice either on chow diet or a 7-month high-fat/high-sucrose diet [49]. In contrast, two other groups reported diet-induced glucose intolerance and insulin resistance in two alternative adiponectin knock-out mouse models after either 2 weeks and 10 weeks of exposure to high fat/high-sucrose diets, respectively [47,48]. Differences in genetic backgrounds and gene targeting strategies may have contributed to these discrepancies. Regardless, all of these groups reported the absence of baseline glucose and insulin dysregulation in adiponectin knock-out mice. Moreover, the deletion of adiponectin in *ob/ob* mice failed to change their glucose levels compared to *ob/ob* control groups [47]. This result was to some extent consistent with our findings, together suggesting that other pathways may compensate for the loss of adiponectin independently of leptin and Arc*Pomc*. Several reports using the same adiponectin knock-out mouse model demonstrated defects in endothelial function, osteoclastogenesis, exercise-induced neurogenesis, muscle contraction, and other parameters [106—109]. These systemic changes may also occur in Arc*Pomc*$^{-/-}$:*Adipoq*$^{-/-}$ mice and potentially explain the lack of metabolic improvement compared to monogenic Arc*Pomc*$^{-/-}$ mice. It is possible that compound Arc*Pomc*$^{-/-}$:*Adipoq*$^{-/-}$ mice may have other physiological defects or different responses to environmental challenges such as cold exposure or high-fat diet, but additional experiments are out of the scope of the current study.

5. CONCLUSIONS

It is commonly accepted that obese humans and rodents have reduced levels of adiponectin. This study provided the first evidence that despite morbid obesity, Arc*Pomc*$^{-/-}$ mice, and in particular female Arc*Pomc*$^{-/-}$ mice, have elevated circulating adiponectin levels. Moreover, our investigation uncovered a previously unknown physiological pathway starting from POMC neurons via the sympathetic nervous system to circulating adiponectin, which clarifies the biological regulation of adiponectin. Early clinical studies demonstrated reduced adiponectin levels in diabetic hypertensive patients. Further investigation revealed that adiponectin is negatively associated with blood pressure even in normotensives without obesity and diabetes [110,111]. Our study demonstrated that it is possible to alter adiponectin levels *in vivo* by modifying sympathetic outflow, thus providing a possible explanation for our clinical observations.

AUTHOR CONTRIBUTIONS

H.Y. and M.J.L. conceived the study, designed the experiments, analyzed the results, and drafted the manuscript. H.Y., K·C., G.J., Z.T., S·K., and G.S. conducted the experiments. All of the authors edited and approved the final manuscript.

CONFLICT OF INTEREST

None declared.

APPENDIX A. SUPPLEMENTARY DATA

Supplementary data to this article can be found online at https://doi.org/10.1016/j.molmet.2020.01.021.

REFERENCES

[1] Cone, R.D., 2005. Anatomy and regulation of the central melanocortin system. Nature Neuroscience 8(5):571—578.

[2] Mercer, A.J., Hentges, S.T., Meshul, C.K., Low, M.J., 2013. Unraveling the central proopiomelanocortin neural circuits. Frontiers in Neuroscience 7:19.

[3] Obici, S., Feng, Z., Tan, J., Liu, L., Karkanias, G., Rossetti, L., 2001. Central melanocortin receptors regulate insulin action. Journal of Clinical Investigation 108(7):1079—1085.

[4] Costa, J.L., Hochgeschwender, U., Brennan, M., 2006. The role of melanocyte-stimulating hormone in insulin resistance and type 2 diabetes mellitus. Treatments in Endocrinology 5(1):7—13.

[5] Hill, J.W., Faulkner, L.D., 2017. The role of the melanocortin system in metabolic disease: new developments and advances. Neuroendocrinology 104(4):330—346.

[6] Lam, D.D., de Souza, F.S., Nasif, S., Yamashita, M., Lopez-Leal, R., Otero-Corchon, V., et al., 2015. Partially redundant enhancers cooperatively maintain Mammalian pomc expression above a critical functional threshold. PLoS Genetics 11(2):e1004935.

[7] Krude, H., Biebermann, H., Luck, W., Horn, R., Brabant, G., Gruters, A., 1998. Severe early-onset obesity, adrenal insufficiency and red hair pigmentation caused by POMC mutations in humans. Nature Genetics 19(2):155—157.

[8] Mencarelli, M., Walker, G.E., Maestrini, S., Alberti, L., Verti, B., Brunani, A., et al., 2008. Sporadic mutations in melanocortin receptor 3 in morbid obese individuals. European Journal of Human Genetics 16(5):581—586.

[9] Lee, Y.S., Poh, L.K., Kek, B.L., Loke, K.Y., 2008. Novel melanocortin 4 receptor gene mutations in severely obese children. Clinical Endocrinology 68(4):529—535.

[10] Yeo, G.S., Farooqi, I.S., Aminian, S., Halsall, D.J., Stanhope, R.G., O'Rahilly, S., 1998. A frameshift mutation in MC4R associated with dominantly inherited human obesity. Nature Genetics 20(2):111—112.

[11] Yao, T., Deng, Z., Gao, Y., Sun, J., Kong, X., Huang, Y., et al., 2017. Ire1alpha in pomc neurons is required for thermogenesis and glycemia. Diabetes 66(3):663—673.

[12] Martinez-Lopez, N., Garcia-Macia, M., Sahu, S., Athonvarangkul, D., Liebling, E., Merlo, P., et al., 2016. Autophagy in the CNS and periphery coordinate lipophagy and lipolysis in the Brown adipose tissue and liver. Cell Metabolism 23(1):113—127.

[13] Dodd, G.T., Decherf, S., Loh, K., Simonds, S.E., Wiede, F., Balland, E., et al., 2015. Leptin and insulin act on POMC neurons to promote the browning of white fat. Cell 160(1—2):88—104.

[14] Zhang, W., Bi, S., 2015. Hypothalamic regulation of Brown adipose tissue thermogenesis and energy homeostasis. Frontiers in Endocrinology 6:136.

[15] Jiang, H., Ding, X., Cao, Y., Wang, H., Zeng, W., 2017. Dense intra-adipose sympathetic arborizations are essential for cold-induced beiging of mouse white adipose tissue. Cell Metabolism 26(4):686—692 e683.

[16] Song, C.K., Vaughan, C.H., Keen-Rhinehart, E., Harris, R.B., Richard, D., Bartness, T.J., 2008. Melanocortin-4 receptor mRNA expressed in sympathetic outflow neurons to brown adipose tissue: neuroanatomical and functional evidence. American Journal of Physiology - Regulatory, Integrative and Comparative Physiology 295(2):R417—R428.

[17] Song, C.K., Jackson, R.M., Harris, R.B., Richard, D., Bartness, T.J., 2005. Melanocortin-4 receptor mRNA is expressed in sympathetic nervous system outflow neurons to white adipose tissue. American Journal of Physiology - Regulatory, Integrative and Comparative Physiology 289(5):R1467—R1476.

[18] Voss-Andreae, A., Murphy, J.G., Ellacott, K.L., Stuart, R.C., Nillni, E.A., Cone, R.D., et al., 2007. Role of the central melanocortin circuitry in adaptive thermogenesis of brown adipose tissue. Endocrinology 148(4):1550—1560.

[19] Oldfield, B.J., Giles, M.E., Watson, A., Anderson, C., Colvill, L.M., McKinley, M.J., 2002. The neurochemical characterisation of hypothalamic pathways projecting polysynaptically to brown adipose tissue in the rat. Neuroscience 110(3):515—526.

[20] Caron, A., Dungan Lemko, H.M., Castorena, C.M., Fujikawa, T., Lee, S., Lord, C.C., et al., 2018. POMC neurons expressing leptin receptors coordinate metabolic responses to fasting via suppression of leptin levels. Elife 7.

[21] Caron, A., Lee, S., Elmquist, J.K., Gautron, L., 2018. Leptin and brain-adipose crosstalks. Nature Reviews Neuroscience 19(3):153—165.

[22] Scherer, P.E., Williams, S., Fogliano, M., Baldini, G., Lodish, H.F., 1995. A novel serum protein similar to C1q, produced exclusively in adipocytes. Journal of Biological Chemistry 270(45):26746—26749.

[23] Combs, T.P., Berg, A.H., Rajala, M.W., Klebanov, S., Iyengar, P., Jimenez-Chillaron, J.C., et al., 2003. Sexual differentiation, pregnancy, calorie restriction, and aging affect the adipocyte-specific secretory protein adiponectin. Diabetes 52(2):268—276.

[24] Gui, Y., Silha, J.V., Murphy, L.J., 2004. Sexual dimorphism and regulation of resistin, adiponectin, and leptin expression in the mouse. Obesity Research 12(9):1481—1491.

[25] Schraw, T., Wang, Z.V., Halberg, N., Hawkins, M., Scherer, P.E., 2008. Plasma adiponectin complexes have distinct biochemical characteristics. Endocrinology 149(5):2270—2282.

[26] Wang, Z.V., Scherer, P.E., 2016. Adiponectin, the past two decades. Journal of Molecular Cell Biology 8(2):93—100.

[27] Zhu, N., Pankow, J.S., Ballantyne, C.M., Couper, D., Hoogeveen, R.C., Pereira, M., et al., 2010. High-molecular-weight adiponectin and the risk of type 2 diabetes in the ARIC study. Journal of Clinical Endocrinology & Metabolism 95(11):5097—5104.

[28] Goto, M., Goto, A., Morita, A., Deura, K., Sasaki, S., Aiba, N., et al., 2014. Low-molecular-weight adiponectin and high-molecular-weight adiponectin levels in relation to diabetes. Obesity 22(2):401—407.

[29] Fisher, F.M., Trujillo, M.E., Hanif, W., Barnett, A.H., McTernan, P.G., Scherer, P.E., et al., 2005. Serum high molecular weight complex of

adiponectin correlates better with glucose tolerance than total serum adiponectin in Indo-Asian males. Diabetologia 48(6):1084—1087.

[30] Hara, K., Horikoshi, M., Yamauchi, T., Yago, H., Miyazaki, O., Ebinuma, H., et al., 2006. Measurement of the high-molecular weight form of adiponectin in plasma is useful for the prediction of insulin resistance and metabolic syndrome. Diabetes Care 29(6):1357—1362.

[31] Pajvani, U.B., Du, X., Combs, T.P., Berg, A.H., Rajala, M.W., Schulthess, T., et al., 2003. Structure-function studies of the adipocyte-secreted hormone Acrp30/adiponectin. Implications fpr metabolic regulation and bioactivity. Journal of Biological Chemistry 278(11):9073—9085.

[32] Calton, E.K., Miller, V.S., Soares, M.J., 2013. Factors determining the risk of the metabolic syndrome: is there a central role for adiponectin? European Journal of Clinical Nutrition 67(5):485—491.

[33] Yilmaz, M.I., Sonmez, A., Acikel, C., Celik, T., Bingol, N., Pinar, M., et al., 2004. Adiponectin may play a part in the pathogenesis of diabetic retinopathy. European Journal of Endocrinology 151(1):135—140.

[34] Menon, V., Li, L., Wang, X., Greene, T., Balakrishnan, V., Madero, M., et al., 2006. Adiponectin and mortality in patients with chronic kidney disease. Journal of the American Society of Nephrology 17(9):2599—2606.

[35] Klein, B.E., 2007. Overview of epidemiologic studies of diabetic retinopathy. Ophthalmic Epidemiology 14(4):179—183.

[36] Ouchi, N., Kihara, S., Funahashi, T., Matsuzawa, Y., Walsh, K., 2003. Obesity, adiponectin and vascular inflammatory disease. Current Opinion in Lipidology 14(6):561—566.

[37] Matsuda, M., Shimomura, I., 2014. Roles of adiponectin and oxidative stress in obesity-associated metabolic and cardiovascular diseases. Reviews in Endocrine & Metabolic Disorders 15(1):1—10.

[38] Surmacz, E., 2013. Leptin and adiponectin: emerging therapeutic targets in breast cancer. Journal of Mammary Gland Biology and Neoplasia 18(3—4): 321—332.

[39] Vasseur, F., Helbecque, N., Dina, C., Lobbens, S., Delannoy, V., Gaget, S., et al., 2002. Single-nucleotide polymorphism haplotypes in the both proximal promoter and exon 3 of the APM1 gene modulate adipocyte-secreted adiponectin hormone levels and contribute to the genetic risk for type 2 diabetes in French Caucasians. Human Molecular Genetics 11(21):2607—2614.

[40] Vionnet, N., Hani, E.H., Dupont, S., Gallina, S., Francke, S., Dotte, S., et al., 2000. Genomewide search for type 2 diabetes-susceptibility genes in French whites: evidence for a novel susceptibility locus for early-onset diabetes on chromosome 3q27-qter and independent replication of a type 2-diabetes locus on chromosome 1q21-q24. The American Journal of Human Genetics 67(6):1470—1480.

[41] Hara, K., Boutin, P., Mori, Y., Tobe, K., Dina, C., Yasuda, K., et al., 2002. Genetic variation in the gene encoding adiponectin is associated with an increased risk of type 2 diabetes in the Japanese population. Diabetes 51(2): 536—540.

[42] Perez-Martinez, P., Lopez-Miranda, J., Cruz-Teno, C., Delgado-Lista, J., Jimenez-Gomez, Y., Fernandez, J.M., et al., 2008. Adiponectin gene variants are associated with insulin sensitivity in response to dietary fat consumption in Caucasian men. Journal of Nutrition 138(9):1609—1614.

[43] Warren, L.L., Li, L., Nelson, M.R., Ehm, M.G., Shen, J., Fraser, D.J., et al., 2012. Deep resequencing unveils genetic architecture of adipoq and identifies a novel low-frequency variant strongly associated with adiponectin variation. Diabetes 61(5):1297—1301.

[44] Kim, J.Y., van de Wall, E., Laplante, M., Azzara, A., Trujillo, M.E., Hofmann, S.M., et al., 2007. Obesity-associated improvements in metabolic profile through expansion of adipose tissue. Journal of Clinical Investigation 117(9):2621—2637.

[45] Yamauchi, T., Kamon, J., Waki, H., Terauchi, Y., Kubota, N., Hara, K., et al., 2001. The fat-derived hormone adiponectin reverses insulin resistance associated with both lipoatrophy and obesity. Nature Medicine 7(8):941—946.

[46] Combs, T.P., Berg, A.H., Obici, S., Scherer, P.E., Rossetti, L., 2001. Endogenous glucose production is inhibited by the adipose-derived protein Acrp30. Journal of Clinical Investigation 108(12):1875—1881.

[47] Nawrocki, A.R., Rajala, M.W., Tomas, E., Pajvani, U.B., Saha, A.K., Trumbauer, M.E., et al., 2006. Mice lacking adiponectin show decreased hepatic insulin sensitivity and reduced responsiveness to peroxisome proliferator-activated receptor gamma agonists. Journal of Biological Chemistry 281(5):2654—2660.

[48] Maeda, N., Shimomura, I., Kishida, K., Nishizawa, H., Matsuda, M., Nagaretani, H., et al., 2002. Diet-induced insulin resistance in mice lacking adiponectin/ACRP30. Nature Medicine 8(7):731—737.

[49] Ma, K., Cabrero, A., Saha, P.K., Kojima, H., Li, L., Chang, B.H., et al., 2002. Increased beta -oxidation but no insulin resistance or glucose intolerance in mice lacking adiponectin. Journal of Biological Chemistry 277(38):34658—34661.

[50] Hu, E., Liang, P., Spiegelman, B.M., 1996. Adipoq is a novel adipose-specific gene dysregulated in obesity. Journal of Biological Chemistry 271(18): 10697—10703.

[51] Arita, Y., Kihara, S., Ouchi, N., Takahashi, M., Maeda, K., Miyagawa, J., et al., 1999. Paradoxical decrease of an adipose-specific protein, adiponectin, in obesity. Biochemical and Biophysical Research Communications 257(1):79—83.

[52] Daniele, A., Cammarata, R., Masullo, M., Nerone, G., Finamore, F., D'Andrea, M., et al., 2008. Analysis of adiponectin gene and comparison of its expression in two different pig breeds. Obesity 16(8):1869—1874.

[53] Engeli, S., Feldpausch, M., Gorzelniak, K., Hartwig, F., Heintze, U., Janke, J., et al., 2003. Association between adiponectin and mediators of inflammation in obese women. Diabetes 52(4):942—947.

[54] Combs, T.P., Wagner, J.A., Berger, J., Doebber, T., Wang, W.J., Zhang, B.B., et al., 2002. Induction of adipocyte complement-related protein of 30 kilodaltons by PPARgamma agonists: a potential mechanism of insulin sensitization. Endocrinology 143(3):998—1007.

[55] Chhabra, K.H., Adams, J.M., Jones, G.L., Yamashita, M., Schlapschy, M., Skerra, A., et al., 2016. Reprogramming the body weight set point by a reciprocal interaction of hypothalamic leptin sensitivity and Pomc gene expression reverts extreme obesity. Mol Metab 5(10):869—881.

[56] Berglund, E.D., Liu, C., Sohn, J.W., Liu, T., Kim, M.H., Lee, C.E., et al., 2013. Serotonin 2C receptors in pro-opiomelanocortin neurons regulate energy and glucose homeostasis. Journal of Clinical Investigation 123(12):5061—5070.

[57] Bumaschny, V.F., Yamashita, M., Casas-Cordero, R., Otero-Corchon, V., de Souza, F.S., Rubinstein, M., et al., 2012. Obesity-programmed mice are rescued by early genetic intervention. Journal of Clinical Investigation 122(11):4203—4212.

[58] Mori, H., Yao, Y., Learman, B.S., Kurozumi, K., Ishida, J., Ramakrishnan, S.K., et al., 2016. Induction of WNT11 by hypoxia and hypoxia-inducible factor-1alpha regulates cell proliferation, migration and invasion. Scientific Reports 6:21520.

[59] Mori, H., Prestwich, T.C., Reid, M.A., Longo, K.A., Gerin, I., Cawthorn, W.P., et al., 2012. Secreted frizzled-related protein 5 suppresses adipocyte mitochondrial metabolism through WNT inhibition. Journal of Clinical Investigation 122(7):2405—2416.

[60] Hemati, N., Ross, S.E., Erickson, R.L., Groblewski, G.E., MacDougald, O.A., 1997. Signaling pathways through which insulin regulates CCAAT/enhancer binding protein alpha (C/EBPalpha) phosphorylation and gene expression in 3T3-L1 adipocytes. Correlation with GLUT4 gene expression. Journal of Biological Chemistry 272(41):25913—25919.

[61] Chhabra, K.H., Adams, J.M., Fagel, B., Lam, D.D., Qi, N., Rubinstein, M., et al., 2016. Hypothalamic POMC deficiency improves glucose tolerance despite insulin resistance by increasing glycosuria. Diabetes 65(3):660—672.

[62] Chhabra, K.H., Morgan, D.A., Tooke, B.P., Adams, J.M., Rahmouni, K., Low, M.J., 2017. Reduced renal sympathetic nerve activity contributes to

elevated glycosuria and improved glucose tolerance in hypothalamus-specific Pomc knockout mice. Mol Metab 6(10):1274—1285.

[63] Bluher, S., Ziotopoulou, M., Bullen Jr., J.W., Moschos, S.J., Ungsunan, L., Kokkotou, E., et al., 2004. Responsiveness to peripherally administered melanocortins in lean and obese mice. Diabetes 53(1):82—90.

[64] Banno, R., Arima, H., Hayashi, M., Goto, M., Watanabe, M., Sato, I., et al., 2007. Central administration of melanocortin agonist increased insulin sensitivity in diet-induced obese rats. FEBS Letters 581(6):1131—1136.

[65] Marsh, D.J., Hollopeter, G., Huszar, D., Laufer, R., Yagaloff, K.A., Fisher, S.L., et al., 1999. Response of melanocortin-4 receptor-deficient mice to anorectic and orexigenic peptides. Nature Genetics 21(1):119—122.

[66] Perez-Tilve, D., Hofmann, S.M., Basford, J., Nogueiras, R., Pfluger, P.T., Patterson, J.T., et al., 2010. Melanocortin signaling in the CNS directly regulates circulating cholesterol. Nature Neuroscience 13(7):877—882.

[67] Boston, B.A., Cone, R.D., 1996. Characterization of melanocortin receptor subtype expression in murine adipose tissues and in the 3T3-L1 cell line. Endocrinology 137(5):2043—2050.

[68] Haskell-Luevano, C., Lim, S., Yuan, W., Cone, R.D., Hruby, V.J., 2000. Structure activity studies of the melanocortin antagonist SHU9119 modified at the 6, 7, 8, and 9 positions. Peptides 21(1):49—57.

[69] Boston, B.A., 1999. The role of melanocortins in adipocyte function. Annals of the New York Academy of Sciences 885:75—84.

[70] Bradley, R.L., Mansfield, J.P., Maratos-Flier, E., 2005. Neuropeptides, including neuropeptide Y and melanocortins, mediate lipolysis in murine adipocytes. Obesity Research 13(4):653—661.

[71] Adams, J.M., 2015. A physiological role for hypothalamic proopiomelano-cortin in the intrinsic regulation of locomotor activity and stress. Ann Arbor (MI): University of Michigan.

[72] Haynes, W.G., Morgan, D.A., Djalali, A., Sivitz, W.I., Mark, A.L., 1999. Interactions between the melanocortin system and leptin in control of sympathetic nerve traffic. Hypertension 33(1 Pt 2):542—547.

[73] Brito, M.N., Brito, N.A., Baro, D.J., Song, C.K., Bartness, T.J., 2007. Differential activation of the sympathetic innervation of adipose tissues by melanocortin receptor stimulation. Endocrinology 148(11):5339—5347.

[74] Yasuda, T., Masaki, T., Kakuma, T., Yoshimatsu, H., 2004. Hypothalamic melanocortin system regulates sympathetic nerve activity in brown adipose tissue. Experimental Biology and Medicine 229(3):235—239.

[75] Imai, J., Katagiri, H., Yamada, T., Ishigaki, Y., Ogihara, T., Uno, K., et al., 2006. Cold exposure suppresses serum adiponectin levels through sympathetic nerve activation in mice. Obesity 14(7):1132—1141.

[76] Delporte, M.L., Funahashi, T., Takahashi, M., Matsuzawa, Y., Brichard, S.M., 2002. Pre- and post-translational negative effect of beta-adrenoceptor agonists on adiponectin secretion: in vitro and in vivo studies. Biochemical Journal 367(Pt 3):677—685.

[77] Fu, L., Isobe, K., Zeng, Q., Suzukawa, K., Takekoshi, K., Kawakami, Y., 2007. beta-adrenoceptor agonists downregulate adiponectin, but upregulate adiponectin receptor 2 and tumor necrosis factor-alpha expression in adipocytes. European Journal of Pharmacology 569(1—2):155—162.

[78] Komai, A.M., Musovic, S., Peris, E., Alrifaiy, A., El Hachmane, M.F., Johansson, M., et al., 2016. White adipocyte adiponectin exocytosis is stimulated via beta3-adrenergic signaling and activation of Epac1: catecholamine resistance in obesity and type 2 diabetes. Diabetes 65(11):3301—3313.

[79] Sun, J., Gao, Y., Yao, T., Huang, Y., He, Z., Kong, X., et al., 2016. Adiponectin potentiates the acute effects of leptin in arcuate Pomc neurons. Mol Metab 5(10):882—891.

[80] Suyama, S., Maekawa, F., Maejima, Y., Kubota, N., Kadowaki, T., Yada, T., 2016. Glucose level determines excitatory or inhibitory effects of adiponectin on arcuate POMC neuron activity and feeding. Scientific Reports 6:30796.

[81] Ellacott, K.L., Cone, R.D., 2006. The role of the central melanocortin system in the regulation of food intake and energy homeostasis: lessons from mouse models. Philosophical Transactions of the Royal Society of London B Biological Sciences 361(1471):1265—1274.

[82] Ste Marie, L., Miura, G.I., Marsh, D.J., Yagaloff, K., Palmiter, R.D., 2000. A metabolic defect promotes obesity in mice lacking melanocortin-4 receptors. Proceedings of the National Academy of Sciences of the U S A 97(22):12339—12344.

[83] Feng, N., Young, S.F., Aguilera, G., Puricelli, E., Adler-Wailes, D.C., Sebring, N.G., et al., 2005. Co-occurrence of two partially inactivating polymorphisms of MC3R is associated with pediatric-onset obesity. Diabetes 54(9):2663—2667.

[84] Lee, B., Koo, J., Yun Jun, J., Gavrilova, O., Lee, Y., Seo, A.Y., et al., 2016. A mouse model for a partially inactive obesity-associated human MC3R variant. Nature Communications 7:10522.

[85] Haqq, A.M., Muehlbauer, M., Svetkey, L.P., Newgard, C.B., Purnell, J.Q., Grambow, S.C., et al., 2007. Altered distribution of adiponectin isoforms in children with Prader-Willi syndrome (PWS): association with insulin sensitivity and circulating satiety peptide hormones. Clinical Endocrinology 67(6):944—951.

[86] Pravdivyi, I., Ballanyi, K., Colmers, W.F., Wevrick, R., 2015. Progressive postnatal decline in leptin sensitivity of arcuate hypothalamic neurons in the Magel2-null mouse model of Prader-Willi syndrome. Human Molecular Genetics 24(15):4276—4283.

[87] Burnett, L.C., LeDuc, C.A., Sulsona, C.R., Paull, D., Rausch, R., Eddiry, S., et al., 2017. Deficiency in prohormone convertase PC1 impairs prohormone processing in Prader-Willi syndrome. Journal of Clinical Investigation 127(1):293—305.

[88] Maillard, J., Park, S., Croizier, S., Vanacker, C., Cook, J.H., Prevot, V., et al., 2016. Loss of Magel2 impairs the development of hypothalamic Anorexigenic circuits. Human Molecular Genetics 25(15):3208—3215.

[89] Lim, C.Y., Hong, W., Han, W., 2015. Adiponectin is released via a unique regulated exocytosis pathway from a pre-formed vesicle pool on insulin stimulation. Biochemical Journal 471(3):381—389.

[90] Ryu, V., Buettner, C., 2019. Fat cells gobbling up norepinephrine? PLoS Biology 17(2):e3000138.

[91] Tong, Y., Zhao, H.F., Labrie, F., Pelletier, G., 1990. Regulation of proopiomelanocortin messenger ribonucleic acid content by sex steroids in the arcuate nucleus of the female rat brain. Neuroscience Letters 112(1):104—108.

[92] de Souza, F.S., Nasif, S., Lopez-Leal, R., Levi, D.H., Low, M.J., Rubinsten, M., 2011. The estrogen receptor alpha colocalizes with proopiomelanocortin in hypothalamic neurons and binds to a conserved motif present in the neuron-specific enhancer nPE2. European Journal of Pharmacology 660(1):181—187.

[93] Xu, Y., Nedungadi, T.P., Zhu, L., Sobhani, N., Irani, B.G., Davis, K.E., et al., 2011. Distinct hypothalamic neurons mediate estrogenic effects on energy homeostasis and reproduction. Cell Metabolism 14(4):453—465.

[94] Steyn, F.J., Ngo, S.T., Chen, V.P., Bailey-Downs, L.C., Xie, T.Y., Ghadami, M., et al., 2018. 17alpha-estradiol acts through hypothalamic pro-opiomelanocortin expressing neurons to reduce feeding behavior. Aging Cell 17(1).

[95] Nishizawa, H., Shimomura, I., Kishida, K., Maeda, N., Kuriyama, H., Nagaretani, H., et al., 2002. Androgens decrease plasma adiponectin, an insulin-sensitizing adipocyte-derived protein. Diabetes 51(9):2734—2741.

[96] Wang, C., He, Y., Xu, P., Yang, Y., Saito, K., Xia, Y., et al., 2018. TAp63 contributes to sexual dimorphism in POMC neuron functions and energy homeostasis. Nature Communications 9(1):1544.

[97] Burke, L.K., Doslikova, B., D'Agostino, G., Greenwald-Yarnell, M., Georgescu, T., Chianese, R., et al., 2016. Sex difference in physical activity, energy expenditure and obesity driven by a subpopulation of hypothalamic POMC neurons. Mol Metab 5(3):245—252.

[98] Fernandez-Marcos, P.J., Auwerx, J., 2011. Regulation of PGC-1alpha, a nodal regulator of mitochondrial biogenesis. American Journal of Clinical Nutrition 93(4):884S—890S.

[99] Hinojosa-Laborde, C., Chapa, I., Lange, D., Haywood, J.R., 1999. Gender differences in sympathetic nervous system regulation. Clinical and Experimental Pharmacology and Physiology 26(2):122—126.

[100] Dart, A.M., Du, X.J., Kingwell, B.A., 2002. Gender, sex hormones and autonomic nervous control of the cardiovascular system. Cardiovascular Research 53(3):678—687.

[101] Ye, R., Wang, Q.A., Tao, C., Vishvanath, L., Shao, M., McDonald, J.G., et al., 2015. Impact of tamoxifen on adipocyte lineage tracing: inducer of adipogenesis and prolonged nuclear translocation of Cre recombinase. Mol Metab 4(11):771—778.

[102] Liu, L., Zou, P., Zheng, L., Linarelli, L.E., Amarell, S., Passaro, A., et al., 2015. Tamoxifen reduces fat mass by boosting reactive oxygen species. Cell Death & Disease 6:e1586.

[103] Zhao, L., Wang, B., Gomez, N.A., de Avila, J.M., Zhu, M.J., Du, M., 2020. Even a low dose of tamoxifen profoundly induces adipose tissue browning in female mice. International Journal of Obesity 44(1):226—234.

[104] Hesselbarth, N., Pettinelli, C., Gericke, M., Berger, C., Kunath, A., Stumvoll, M., et al., 2015. Tamoxifen affects glucose and lipid metabolism parameters, causes browning of subcutaneous adipose tissue and transient body composition changes in C57BL/6NTac mice. Biochemical and Biophysical Research Communications 464(3):724—729.

[105] Berg, A.H., Combs, T.P., Du, X., Brownlee, M., Scherer, P.E., 2001. The adipocyte-secreted protein Acrp30 enhances hepatic insulin action. Nature Medicine 7(8):947—953.

[106] Ouedraogo, R., Gong, Y., Berzins, B., Wu, X., Mahadev, K., Hough, K., et al., 2007. Adiponectin deficiency increases leukocyte-endothelium interactions via upregulation of endothelial cell adhesion molecules in vivo. Journal of Clinical Investigation 117(6):1718—1726.

[107] Krause, M.P., Liu, Y., Vu, V., Chan, L., Xu, A., Riddell, M.C., et al., 2008. Adiponectin is expressed by skeletal muscle fibers and influences muscle phenotype and function. American Journal of Physiology - Cell Physiology 295(1):C203—C212.

[108] Tu, Q., Zhang, J., Dong, L.Q., Saunders, E., Luo, E., Tang, J., et al., 2011. Adiponectin inhibits osteoclastogenesis and bone resorption via APPL1-mediated suppression of Akt1. Journal of Biological Chemistry 286(14):12542—12553.

[109] Yau, S.Y., Li, A., Hoo, R.L., Ching, Y.P., Christie, B.R., Lee, T.M., et al., 2014. Physical exercise-induced hippocampal neurogenesis and antidepressant effects are mediated by the adipocyte hormone adiponectin. Proceedings of the National Academy of Sciences of the U S A 111(44):15810—15815.

[110] Iwashima, Y., Katsuya, T., Ishikawa, K., Ouchi, N., Ohishi, M., Sugimoto, K., et al., 2004. Hypoadiponectinemia is an independent risk factor for hypertension. Hypertension 43(6):1318—1323.

[111] Kim, D.H., Kim, C., Ding, E.L., Townsend, M.K., Lipsitz, L.A., 2013. Adiponectin levels and the risk of hypertension: a systematic review and meta-analysis. Hypertension 62(1):27—32.